General Disclaimer

One or more of the Following Statements may affect this Document

- This document has been reproduced from the best copy furnished by the organizational source. It is being released in the interest of making available as much information as possible.

- This document may contain data, which exceeds the sheet parameters. It was furnished in this condition by the organizational source and is the best copy available.

- This document may contain tone-on-tone or color graphs, charts and/or pictures, which have been reproduced in black and white.

- This document is paginated as submitted by the original source.

- Portions of this document are not fully legible due to the historical nature of some of the material. However, it is the best reproduction available from the original submission.

NATIONAL AERONAUTICS AND SPACE ADMINISTRATION

Technical Memorandum 33-790

Reduction of Gaseous Pollutant Emissions From Gas Turbine Combustors Using Hydrogen-Enriched Jet Fuel—A Progress Report

JET PROPULSION LABORATORY
CALIFORNIA INSTITUTE OF TECHNOLOGY
PASADENA, CALIFORNIA

October 15, 1976

TECHNICAL REPORT STANDARD TITLE PAGE

1. Report No. 33-790	2. Government Accession No.	3. Recipient's Catalog No.
4. Title and Subtitle REDUCTION OF GASEOUS POLLUTANT EMISSIONS FROM GAS TURBINE COMBUSTORS USING HYDROGEN-ENRICHED JET FUEL -- A PROGRESS REPORT		5. Report Date October 15, 1976 6. Performing Organization Code
7. Author(s) Richard M. Clayton		8. Performing Organization Report No.
9. Performing Organization Name and Address JET PROPULSION LABORATORY California Institute of Technology 4800 Oak Grove Drive Pasadena, California 91103		10. Work Unit No. 11. Contract or Grant No. NAS 7-100 13. Type of Report and Period Covered Technical Memorandum
12. Sponsoring Agency Name and Address NATIONAL AERONAUTICS AND SPACE ADMINISTRATION Washington, D.C. 20546		14. Sponsoring Agency Code
15. Supplementary Notes		

16. Abstract

Recent progress in an evaluation of the applicability of the hydrogen-enrichment concept to achieve ultralow gaseous pollutant emissions from gas turbine combustion systems is described. The target emission indexes (g/kg fuel) for the program are 1.0 for oxides of nitrogen (as NO_2) and carbon monoxide, and 0.5 for unburned hydrocarbons. The basic concept utilizes premixed molecular hydrogen, conventional jet-fuel, and air to depress the lean flammability limit of the mixed fuel. This is shown to permit very lean combustion with its low NO_x production while simultaneously providing an increased flame stability margin with which to maintain low CO and HC emissions.

Experimental emission characteristics and selected analytical results are presented for a cylindrical research combustor designed for operation with inlet-air state conditions typical for a 30:1 compression ratio, high-bypass ratio, turbofan commercial aviation engine. The combustor was operated at simulated low, cruise, and takeoff power conditions for this class of engine. Emissions data for H_2/jet-fuel (JP-5) mixes and for jet fuel only are presented for a wide range of equivalence ratio for the low and cruise power conditions. However, lack of flameholder durability precluded operating the combustor with H_2 at the takeoff power condition. Further burner

17. Key Words (Selected by Author(s))	18. Distribution Statement
Aircraft Propulsion and Power Propellants and Fuels	Unclassified -- Unlimited

19. Security Classif. (of this report)	20. Security Classif. (of this page)	21. No. of Pages	22. Price
Unclassified	Unclassified	52	

TECHNICAL REPORT STANDARD TITLE PAGE

1. Report No. 33-790	2. Government Accession No.	3. Recipient's Catalog No.
4. Title and Subtitle		5. Report Date
		6. Performing Organization Code
7. Author(s)		8. Performing Organization Report No.
9. Performing Organization Name and Address JET PROPULSION LABORATORY California Institute of Technology 4800 Oak Grove Drive Pasadena, California 91103		10. Work Unit No. 11. Contract or Grant No. NAS 7-100 13. Type of Report and Period Covered
12. Sponsoring Agency Name and Address NATIONAL AERONAUTICS AND SPACE ADMINISTRATION Washington, D.C. 20546		14. Sponsoring Agency Code
15. Supplementary Notes		

16. Abstract

development is required to demonstrate the concept at this severe operating condition.

The ultralow-emission goals were simultaneously achieved for the cruise power condition at an average burning equivalence ratio of 0.38 using 10-12 mass % H_2 in the total fuel. The emission goals were not achievable with jet fuel alone, due to the onset of lean blowout at too high an equivalence ratio to sufficiently reduce the NO_x emission. The emission goals were not achieved simultaneously for the low power condition, but any two of the three goals were achievable in the equivalence ratio range of 0.3 to 0.4 with a relatively small residual in the third. About 15% H_2 was required.

On the basis of the present results, it is concluded that H_2-enrichment is feasible to implement, given further dedicated development. Intermediate steps in this development for the ongoing evaluation program are to improve premixing homogeneity and flameholder design. The ultimate major step is demonstrating the feasibility of on-board hydrogen generation.

17. Key Words (Selected by Author(s))	18. Distribution Statement		
19. Security Classif. (of this report)	20. Security Classif. (of this page)	21. No. of Pages	22. Price

NATIONAL AERONAUTICS AND SPACE ADMINISTRATION

Technical Memorandum 33-790

Reduction of Gaseous Pollutant Emissions From Gas Turbine Combustors Using Hydrogen-Enriched Jet Fuel—A Progress Report

Richard M. Clayton

JET PROPULSION LABORATORY
CALIFORNIA INSTITUTE OF TECHNOLOGY
PASADENA, CALIFORNIA

October 15, 1976

PREFACE

The work described in this report was performed by the Propulsion Division of the Jet Propulsion Laboratory.

ACKNOWLEDGMENT

The author would like to express appreciation to all individuals who have contributed to the initiation and progress of these experiments. Particular acknowledgment is due to Jack H. Rupe, the innovator of the H_2-enrichment concept for pollution control; Roy Bjorklund, test engineer; and Daniel Griffin, instrumentation engineer. The initiative and interest of Robert King and James Arnold, test facility technicians, are also gratefully appreciated.

CONTENTS

FIGURES (contd)

FIGURES (contd)

ABSTRACT

Recent progress in an evaluation of the applicability of the hydrogen-enrichment concept to achieve ultralow gaseous pollutant emissions from gas turbine combustion systems is described. The target emission indexes (g/kg fuel) for the program are 1.0 for oxides of nitrogen (as NO_2) and carbon monoxide, and 0.5 for unburned hydrocarbons. The basic concept utilizes premixed molecular hydrogen, conventional jet-fuel, and air to depress the lean flammability limit of the mixed fuel. This is shown to permit very lean combustion with its low NO_x production while simultaneously providing an increased flame stability margin with which to maintain low CO and HC emissions.

Experimental emission characteristics and selected analytical results are presented for a cylindrical research combustor designed for operation with inlet-air state conditions typical for a 30:1 compression ratio, high-bypass ratio, turbofan commercial aviation engine. The combustor was operated at simulated low, cruise, and takeoff power conditions for this class of engine. Emissions data for H_2/jet-fuel (JP-5) mixes and for jet fuel only are presented for a wide range of equivalence ratio for the low and cruise power conditions. However, lack of flameholder durability precluded operating the combustor with H_2 at the takeoff power condition. Further burner development is required to demonstrate the concept at this severe operating condition.

The ultralow-emission goals were simultaneously achieved for the cruise power condition at an average burning equivalence ratio of 0.38 using 10-12 mass % H_2 in the total fuel. The emission goals were not achievable with jet fuel alone, due to the onset of lean blowout at too high an equivalence ratio to sufficiently reduce the NO_x emission. The emission goals were not achieved simultaneously for the low power condition, but any two of the three goals were achievable in the equivalence ratio range of 0.3 to 0.4 with a relatively small residual in the third. About 15% H_2 was required.

On the basis of the present results, it is concluded that H_2-enrichment is feasible to implement, given further dedicated development. Intermediate steps in this development for the ongoing evaluation program are to improve premixing homogeneity and flameholder design. The ultimate major step is demonstrating the feasibility of on-board hydrogen generation.

I. INTRODUCTION

The reduction of atmospheric pollutant emissions from transportation combustion sources has been a national concern for a number of years. Recently, the aviation community has directed its attention to the problem of reducing such emissions from aircraft gas turbine engines. The technological complexity of the problem is suggested in Ref. 1, which lists 113 titles on the subject to the year 1973. Later summaries of technological status and recent advances are contained in Refs. 2-6.

From a regulatory standpoint, the Environmental Protection Agency (EPA) has established standards (Ref. 7) for aircraft jet engines that, by 1981, will require as much as 65% reduction in emissions of oxides of nitrogen (NO_x) for newly certified engines under takeoff power. Even greater levels of reduction of carbon monoxide (CO) and unburned hydrocarbons (HC) emissions will be required for ground-idle conditions. Moreover, concern over ozone depletion in the stratosphere from NO_x may ultimately lead to very stringent standards for high-altitude cruise operation. And even though it is understood that the NO_x emissions are the result of high combustion temperatures under high-power operation and that CO and HC emissions are the result of reduced combustion efficiency under low-power operation, "conventional" approaches to combustor design changes generally fail to show promise of achieving the emission standards across the engine operating range. This lack of success is inherent in the opposing combustion requirements involved in reducing the two classes of emissions. Thus, the development of new combustor design concepts is required before combustion temperature can be reduced substantially without sacrificing flame stability and combustion efficiency.

In order to advance the technology and to identify promising new concepts, a portion of government-sponsored research has been utilized in exploring schemes to achieve ultralow levels of emissions; i.e., levels considerably lower than the EPA standards. The generally accepted target goals (also adopted for the present JPL work) for ultralow emissions and burner performance are shown in Table 1, where they are compared to certain EPA 1981 standards, to typical production engine emissions, and to results from a portion of the NASA Experimental Clean Combustor Program (ECCP). Data for subsonic cruise is also shown in Table 1, although a standard for this operating mode has not been specified by the EPA.

It is noted that the ECCP target goals (not shown) are of the same order as the EPA 1981 standards: not ultralow goals. Additionally, that work is keyed to combustor design concepts amenable to incorporation in current production engines. Hence, essentially conventional, though highly hybridized, design approaches have been used. The results are shown to illustrate that, although emissions can be significantly reduced, these reductions fall short of the EPA standards. And it remains to be demonstrated that the reductions shown can be retained when the revised design is incorporated in the engine.

Attainment of the ultralow goals for an operational engine would reduce NO_x and CO an order of magnitude below the standards for the Landing-Take-Off (LTO) cycle, a requirement that may never be imposed. However, a significant design margin will be required of any new concept to allow for the inevitable

compromises in performance when the concept is transformed to an operational engine. Certainly the design technology derived from exploration of lower emission limit concepts will ultimately contribute to minimizing pollutants.

The control over peak flame temperature that is available with premixed (includes prevaporized liquid fuel by definition) combustion is well known and, today, this mode of combustion is presumed to be necessary to greater or lesser degree in all advanced combustor concepts for minimizing NO_x production. Several recent investigations have shown the potential of premixed, fuel-lean combustion in laboratory burners for achieving ultralow NO_x emissions (cf. Refs. 8 and 9), but the leanness required (at the higher power inlet air conditions) is seriously close to the lean burning limit of hydrocarbon and air. Thus, the attractiveness of the premixed, lean-burning concept is tempered by the narrow margin between the mixture strength and combustor dwell times required for NO_x control and those required for flame stability, ignition, and high combustion efficiency. Indeed if the ultralow goals for CO and HC listed in Table 1 are retained, the margin is essentially zero.

One concept proposed for increasing this margin is the use of a catalyst bed (Ref. 6). The technique has several attractive features and should receive continued attention. An alternate approach and the subject of this report is the concept of hydrogen-enrichment.

The basic hydrogen-enrichment concept and its application to jet combustors are described in Appendix A. Briefly, the unique lean-burning properties of molecular hydrogen are utilized to depress the lean flammability limit of mixtures of premixed H_2, jet fuel, and air and thus the combustion margin available for pollution control is significantly widened. The concept limit of 100% H_2, premixed with air, would potentially permit burner operation down to idle power with no CO or HC emissions and high-power operations with ultralow levels of NO_x. But use of 100% H_2 is not the essence of the concept because of today's obvious logistical problems with H_2 as a pure fuel. Instead, the object is to use as little H_2 as possible to provide the necessary combustion margin. Effectively, the H_2 replaces a portion of the ordinary jet fuel.

In the broadest view of the concept, the H_2 might be provided by using a two-stage combustion system where a large portion of the total fuel flow to the system would be partially oxidized in the first stage in order to supply a hydrogen-bearing gas stream to the second stage. In the second stage the remainder of the system fuel would be burned lean after premixing with the remainder of the system air and the H_2-bearing product of the first stage.

Hydrogen enrichment for reduction of pollution emissions was originally introduced at this Laboratory in 1973 for application to internal combustion engines, where the advantage of improved thermal efficiency is also available with lean burning. Many of the developments of the concept in application to automotive engines are reported in Refs. 10-13. The concept also is being applied to general aviation piston engines, where a significant extension in flight range (for a fixed fuel load), as well as pollution reduction, is expected (Ref. 14).

The present application of the concept to continuous flow combustors for reducing emissions is the direct outgrowth of the successes of the work cited above. However, the work reported herein has not reached the maturity of an integrated H_2-generation/combustor system. The present objective is to experimentally evaluate the practical feasibility of the concept, using bottled H_2. It is noted that the essential "proof of principle" of the concept as applied to a laboratory pipe burner operating with premixed H_2/propane/air was obtained previously in the interesting experiments of Anderson (Ref. 15).

The practical aspects of the ongoing JPL evaluation are fulfilled by conducting the experiments with inlet-air state conditions typical for 30:1 compression ratio, high-bypass, turbofan commercial aviation engines. Also functionally feasible burner configurations are emphasized that would be amenable to application to future engines with vigorous engineering development. Inlet-air conditions for three power levels have been emphasized to date: low, $4.46 \times 10^5 N/m^2$ (4.4 atm) at 455 K (360°F); cruise, $11.75 \times 10^5 N/m^2$ (11.6 atm) at 728 K (850°F); and takeoff, $30.39 \times 10^5 N/m^2$ (30 atm) at 812 K (1000° F).[1]

Premix homogeneity and complete combustion are the limiting practical considerations in achieving lower-limit pollutant emissions via any lean-burning scheme, whether with hydrogen or not. The present experimental combustor, designated Mod 2, is the second JPL configuration intended to satisfy those requirements and at the same time provide adequate hardware durability to accomplish the experiments. To our knowledge the present work is unique in carrying premix jet burner schemes to the full range of inlet-air pressure and temperature, even with jet fuel alone. And although we have not yet fully succeeded, especially when H_2 is added, considerable progress has been made with the Mod 2 burner.

Emissions data for H_2/jet fuel (JP-5) mixes and for jet fuel only have been obtained over a wide range of equivalence ratio for the low and cruise power conditions. Data with jet fuel alone have been obtained at the takeoff power condition. In no case has the problem of flashback and flameholding in the premixing zone previously encountered in the original (Mod 1) burner been observed (Ref. 16 and Appendix B). However, flameholder durability was a persistent problem that ultimately precluded operating the Mod 2 burner with H_2 at the takeoff power condition.

Four runs have been made at the takeoff condition, three with jet fuel only where time to failure was about 20 min. A fourth and final attempt was aborted when the flameholder failed during purge procedures prior to mixed H_2/jet fuel operation.

The purpose of this report is to document the recent results from the Mod 2 burner experiments. It is anticipated that future work will be separately documented.

---

[1]Where double units are given in this report, the principal measurements and calculations were made in English system units.

II. DESCRIPTION OF EXPERIMENTS

A. MOD 2 BURNER

The design parameters for the burner are summarized in Table 2. Although the burner was not intended to be a scale version of the G.E. CF6-50 combustor, analogous design parameters for a production version are shown for reference. The experimental burner has about 4% of the mass throughput and about 40% of the combustion space rate of the engine combustor.

For testing, the Mod 2 burner is housed within a heavy-walled pressure vessel which also serves as a plenum chamber for the preheated inlet-air supply. (See Appendix B for a description of the test facility.) The burner assembly is shown schematically in Fig. 1 and as installed on the plenum end-dome in Fig. 2. The burner is designed to utilize 100% of the air flow in the combustion process; thus, air film cooling and air dilution which are normally used in an engine combustor are omitted. In this way, combustion effects from air injection are avoided for the concept evaluation. The cylindrical combustion chamber is water cooled, as are the sonic exhaust nozzle and gas sample probe.

The burner is intended to operate with a near-homogeneous fuel/air mixture. This is accomplished in the mixing section where gaseous H_2, finely atomized jet-fuel, and the air are combined. The interfacial component between the combustion and premixing zones is a perforated conical flameholder which distributes th incoming high-velocity mixture across the chamber cross section. The jet flow produced by the perforations results in many small recirculation zones on the downstream side of the flameholder and thus provides flame stabilization. A spark gap located on the downstream side of the flameholder provides ignition but is inactive once steady burning is obtained.

1. Fuel Injection/Premix Section As is seen from Fig. 1, premixing is accomplished via a coaxial flow scheme where the fuels are injected at the bell-mouthed entry to a 5.22-cm (2.07-in.) diameter straight cylindrical tube, 20.32 cm (8.00 in.) long. The flow area provides space velocities ranging from 88 m/s (290 ft/s) to 125 m/s (410 ft/s) for the low power condition, 128 m/s (420 ft/s) to 140 m/s (460 ft/s) for the cruise power condition, and 146 m/s (480 ft/s) to 163 m/s (535 ft/s) for the takeoff power condition. The velocity variation at each condition is the result of adjustments to air flow rate as eqivalence ratio is varied so that near-constant combustion pressure is maintained.

These relatively high velocities and the reasonably short length of the premixing section are utilized to avoid flashback and autoignition in the premixed reactants. Reliable quantitative design requirements to accomplish this under the burner inlet flow and state conditions for modern gas turbine engines are not available in the literature. In any event, the prior experience with the Mod 1 burner (Appendix B), and the fact that H_2 is much more reactive than jet fuel alone, led to conservatism, and the velocity range chosen is based on typical velocities already present at engine compressor discharge. The resulting spatial dwell-time in the premixing section ranges from 3.4 to 1.9 ms from low to takeoff power conditions.

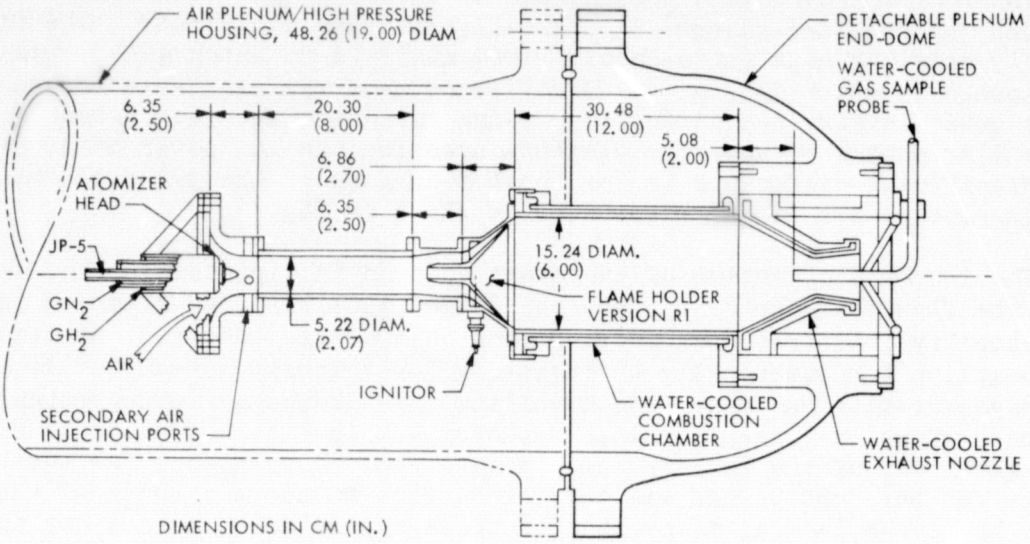

Fig. 1. Mod 2 burner, assembly and test installation

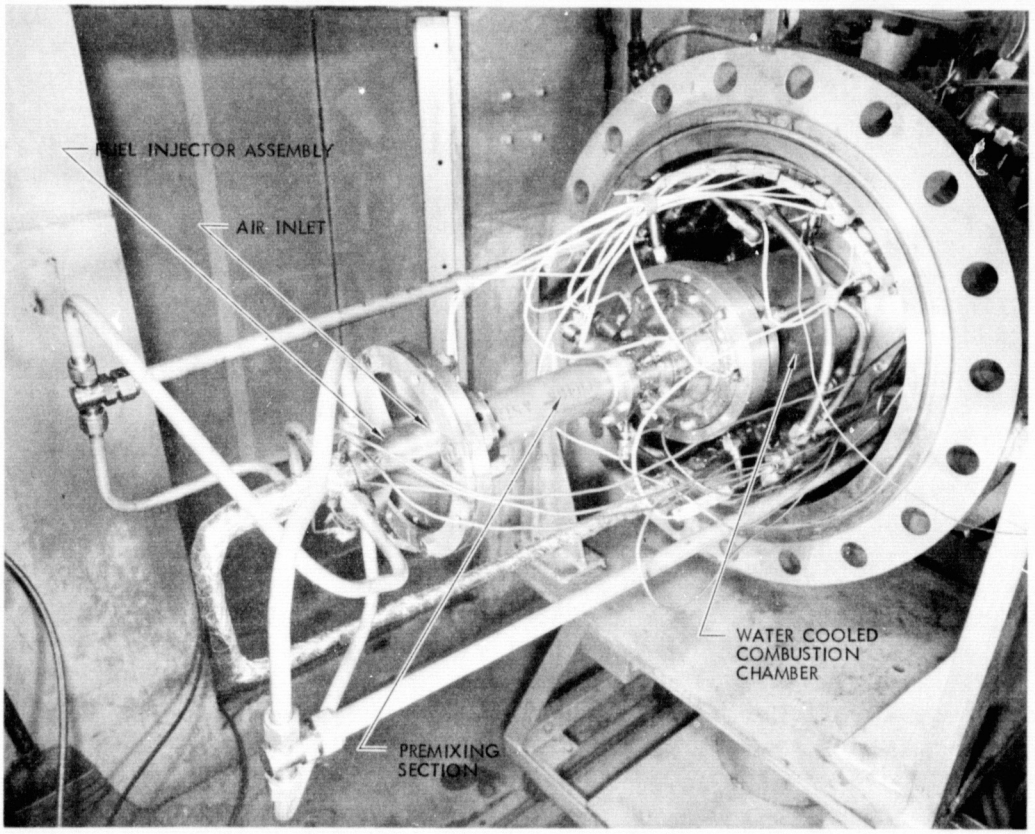

Fig. 2. Mod 2 burner assembly installed in plenum end dome

The fuel injector is a JPL-fabricated device designed to inject finely atomized jet fuel and gaseous H_2 coaxially into the air stream. The injector assembly consists of a three-section feed manifold to which an atomizer head is attached as shown in Fig. 1. A different head was available for each of the power levels, the differences being noted in Fig. 3a. Except for the smaller number of atomizer elements used for the low power head, the only significant difference is the total flow area of the jet-fuel orifices. A photograph of the cruise power head is shown in Fig. 3b.

The intended operation of the atomizer head is depicted in Fig. 4a, where the flow from two of the several symmetrically spaced elements is schematically illustrated on a two-dimensional basis. Jet-fuel atomization is accomplished pneumatically by injecting low-velocity streams of liquid fuel into high-velocity N_2 flow. The resulting fog-like spray is suggested in the short-duration-flash illuminated photograph in Fig. 4b, which shows a water flow test of the takeoff power head. Flow restrictions for the test fixture for this photograph limited the N_2 flow to about a tenth of the design value; hence the lateral dispersion of the spray is greater than for the design condition, which produced a nearly axial flow with injection into quiescent air.

The N_2 design flow was based on maintaining a mass ratio of N_2-to-jet-fuel of unity or greater, with sonic jet velocity. And since it was also chosen to operate the burner with a constant N_2-to-air mass ratio, the N_2 flow rate was fixed by choosing it to equal the jet-fuel flow rate for an equivalence ratio of 0.6. In practice, a nearly constant N_2 mass flow rate of 4 to 5% of the air mass flow rate for all operating conditions was used. This small dilution of the combustion reactants was deemed acceptable in lieu of the addition of a source of supercharged air to the test facility. Kinetic estimates of the effects of this additional N_2 showed no tendency to increase the NO formation rate.

No attempt to measure the drop sizes produced by this atomizer has been made but comparison of the design factors with atomization correlations for other pneumatic atomizers indicates that drop mean diameters in the range of 10-20 μm should be produced. Without allowance for further size reduction from evaporation during passage through the mixer, this size range approaches that where the drops burn essentially as a vapor. Certainly this was the intent and justification for selecting that atomizing scheme.

As is depicted in Fig. 4a, the N_2/jet-fuel flow pattern produced by the pairs of atomizer elements results in a region of high mass flux midway between adjacent fuel delivery tubes. This region is formed by the impingement of the bifurcated N_2 flow from around the tubes and since nearly all the jet fuel must flow through that region, it was chosen to inject the hydrogen there. Thus, an axially directed, subsonic H_2 injection jet was placed at each of those locations. The rationale seems obvious, but it is now recognized that certain impingement dynamics considerations in this flow configuration may be detrimental to good mixing of the H_2 and jet fuel.

The scope of these experiments did not permit a thorough evaluation of the mixing performance of the injector/premixing section. But in ancillary tests prior to commencing combustion runs, wherein some information on the distribution of H_2 was obtained, it was clear that the H_2 tended to be concentrated down

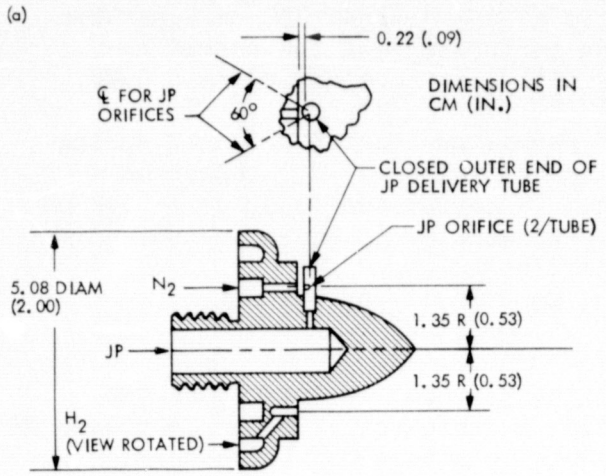

ITEM	ATOMIZER HEAD		
	LOW (L)	CRUISE (C)	TAKEOFF (H)
NUMBER OF EQUALLY SPACED ELEMENTS	10	20	20
ORIFICE DIAM			
JP (TWO/ELEMENT)	.033 (.013)	.036 (.014)	.061 (.024)
N_2	.140 (.055)	.089 (.035)	.089 (.035)
H_2	.178 (.070)	.140 (.055)	.140 (.055)

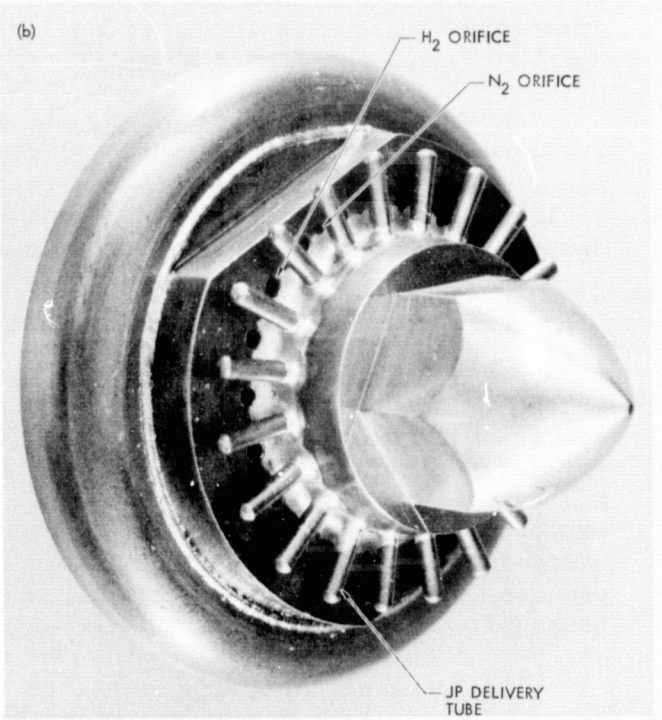

Fig. 3. JPL pneumatic atomizer head

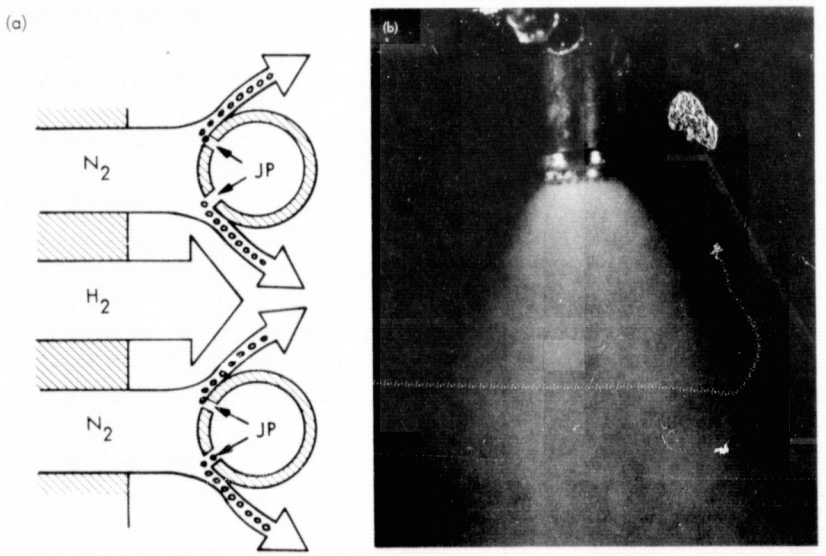

Fig. 4. JPL atomizer head operation

the center of the mixing duct. This was improved but not eliminated by adding four secondary air injection ports near the throat plane of the bell mouth entry (Fig. 1) and this arrangement was used as the "standard" configuration. Apparent deficiencies in the overall mixing performance of the premixing section as deduced from combustion results will be discussed in Section IV.

Only one modification of the standard premixing section was used during the experiments. This consisted of doubling the number of air injection ports in the plane of the existing ones, and in moving the injector ~ 0.48 cm (0.19 in.) further into the entry section. As will be noted later, this change apparently did not improve the mixing.

2. Chamber Inlet and Flameholder Geometry Prior to commencing the pressurized combustion tests reported herein, a series of atmospheric-pressure screening tests was made to choose a flameholding scheme for the burner. The setup for these tests is shown in Fig. 5. A number of swirler designs, a 7.6-cm (3-in.) diameter hollow cone, and a perforated conical baffle were explored. The various candidate components are shown installed in the combustor entry dome in Fig. 6a, b, and c. Suffice it to say that the conical baffle produced the better flame stability and it was subsequently adopted for the pressurized experiments, typically as shown in the burner schematic in Fig. 1.

The baseline design requirements for this scheme were to keep the mixture velocity everywhere across the upstream side of the flameholder and through the flameholder flow area at least equal to the approach velocity from the mixing section, and to distribute the mixture equally across the chamber area. Satisfying the first requirement was intended to maintain mixture velocities well above turbulent flame speeds and to reduce tendencies for flow separation from inertial effects. The annular flow passage between the dome wall and upstream surface of the flameholder was sized to accomplish this in accordance with the progressive outflow from the flameholder perforations and the flow dumped through the annular slit at the skirt edge of the baffle.

The second requirement was met originally by sizing and locating the drilled perforations to inject equal mixture flows into three equal annular areas with the remaining quarter of the total flow dumped at the skirt. This arrangement is the one shown in Fig. 6c, which also shows the single bolt that connected the flameholder to a spider support located just upstream of the apex of the baffle. This flameholder is designated version H. Subsequent variations to the hole pattern favored increased flow through the apex region; however, total blockage remained nearly constant at about 75% of the chamber crosssectional area except for one flameholder version noted later.

All flameholders were fabricated from AISI 310 stainless steel sheet stock, 1.6 mm (0.062 in.) thick.

After the first series of low power runs and the first run at the cruise condition, during which the failure shown in Fig. 7 was typical, the mounting arrangement and flow area distribution in the apex region of the flameholder were revised to strengthen the support and to reduce the hot gas recirculation in the apex region. The revised flameholder (designated R1) is shown in Fig. 8. The support webs were welded into the mounting ring and the entire

assembly was installed in the dome as shown in Fig. 1. The original spider support was thus eliminated although the extended nose piece was used to fill in the space of the spider hub and its fairing. Additional flow was injected into the apex region by inserting a tube through the full length of the nose piece and by moving the inner row of perforations towards the center.

The R1 configuration was used for the bulk of the cruise power tests even though its durability was poor. Typical damage after 2 to 3 hours operation at cruise ranged from complete failure to that shown in Fig. 9a, b, and c. The asymmetrical pattern of damage, particularly the most common as shown in Fig. 9b, was eventually associated with a flow disturbance caused by the ignitor or its feed-through port. This is apparent in the heat stress to the ring in the vicinity of the port shown in Fig. 9c.

This problem area was conclusively established after the initial takeoff power run which was terminated for a different reason after several minutes on condition, but which produced similar flameholder damage to that shown in Fig. 9c. Consequently, the remaining high-power runs were made with the ignitor relocated to a position near the flameholder skirt. This relocation appeared to eliminate that local hot spot. The problem of flameholding in high-temperature, premixed flow disturbances was again observed, however, in a special test at cruise power with the ignitor in its new location, but with several thermocouple wires attached to the upstream flameholder surface and traversing the flow passage. These wires were only 0.5 mm (.020 in.) in diameter, yet a general hot area was noted downstream of them and several of the wires were burned through.

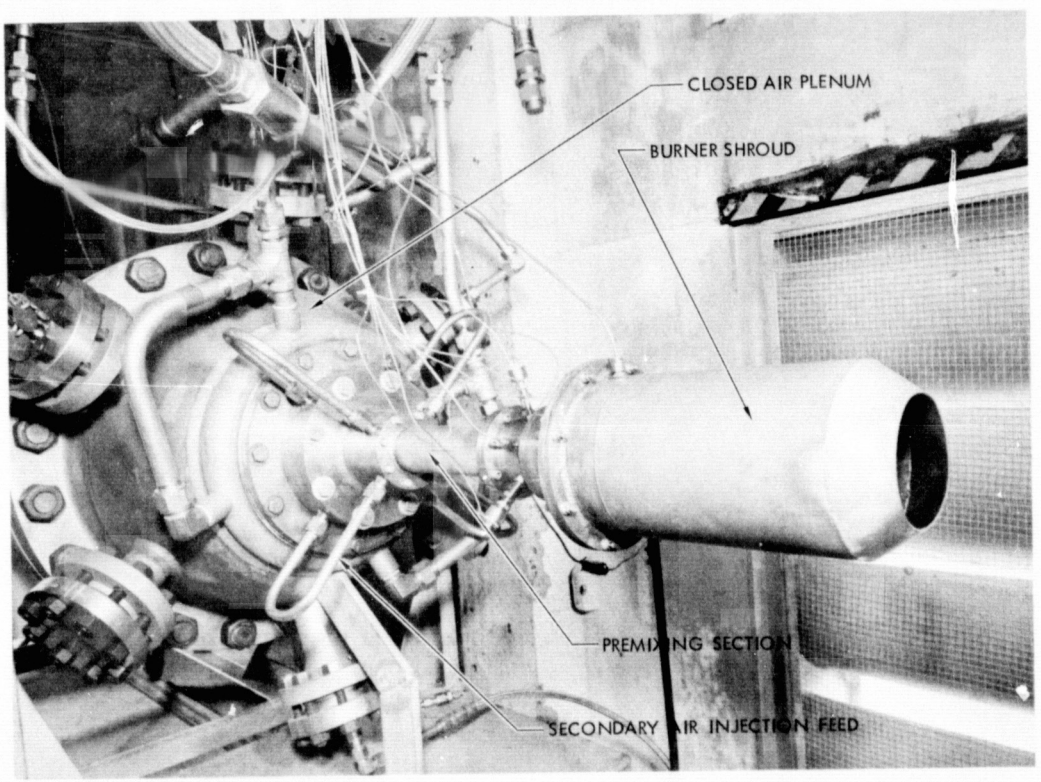

Fig. 5. Mod 2 burner installed for atmospheric pressure tests

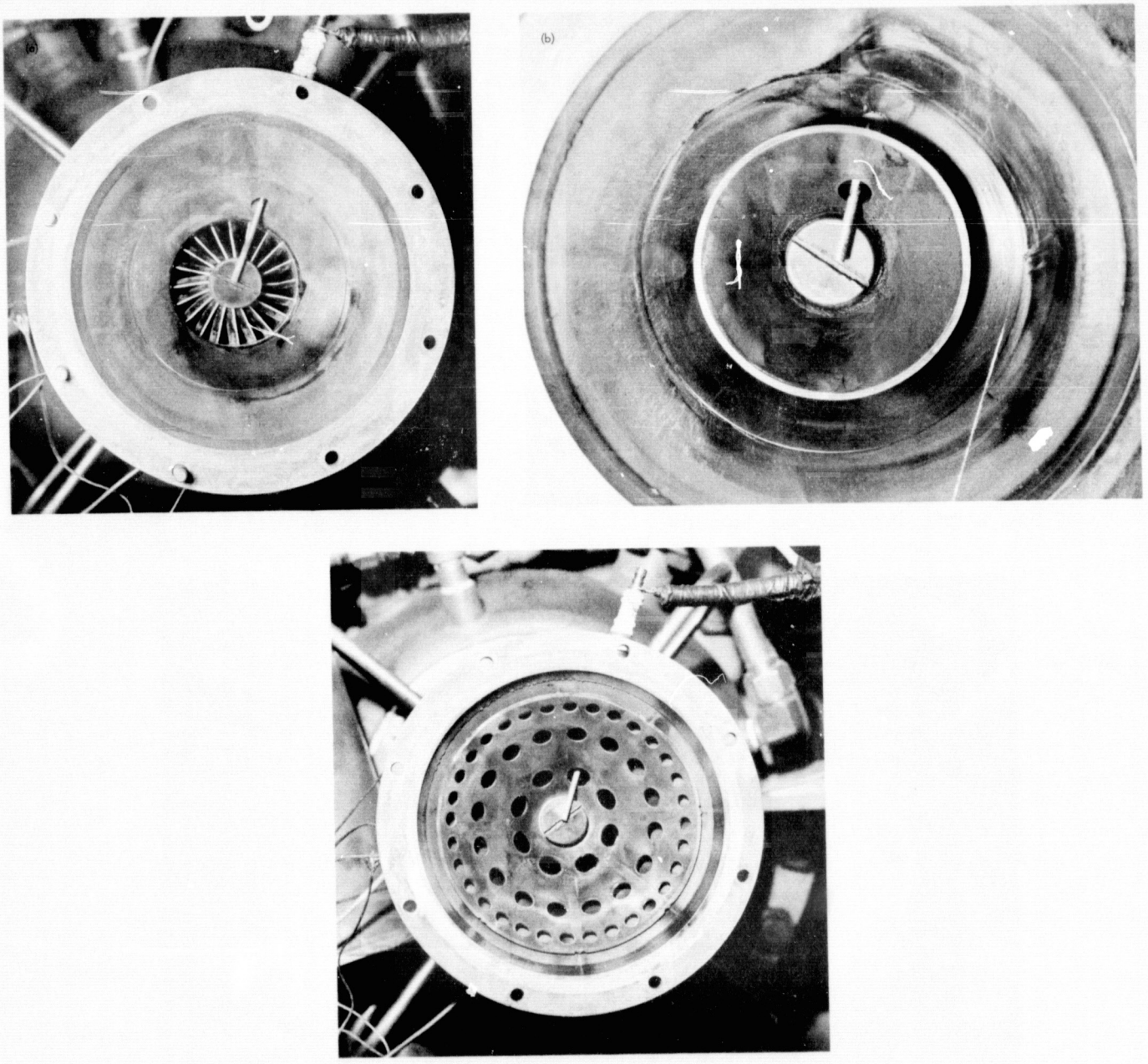

Fig. 6. Flame-holding schemes screened in atmospheric tests

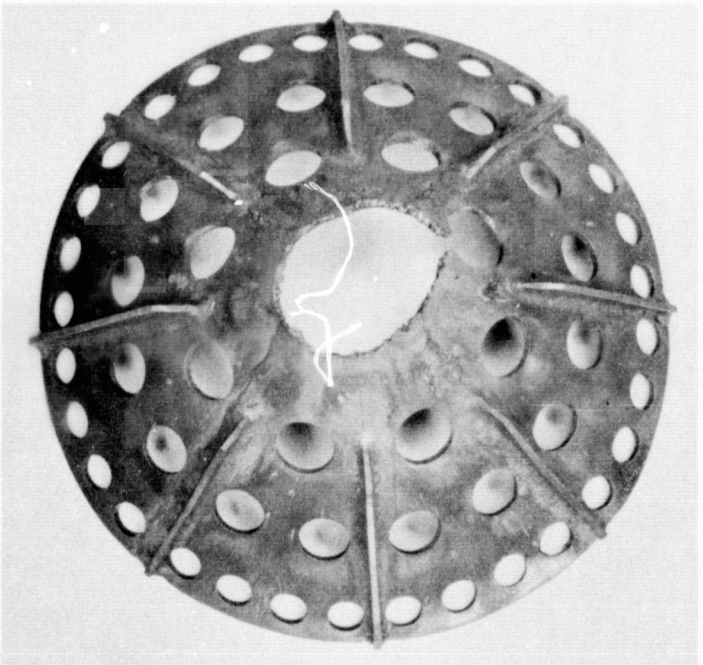

Fig. 7. Typical damage to flameholder H, configurations AL and AC

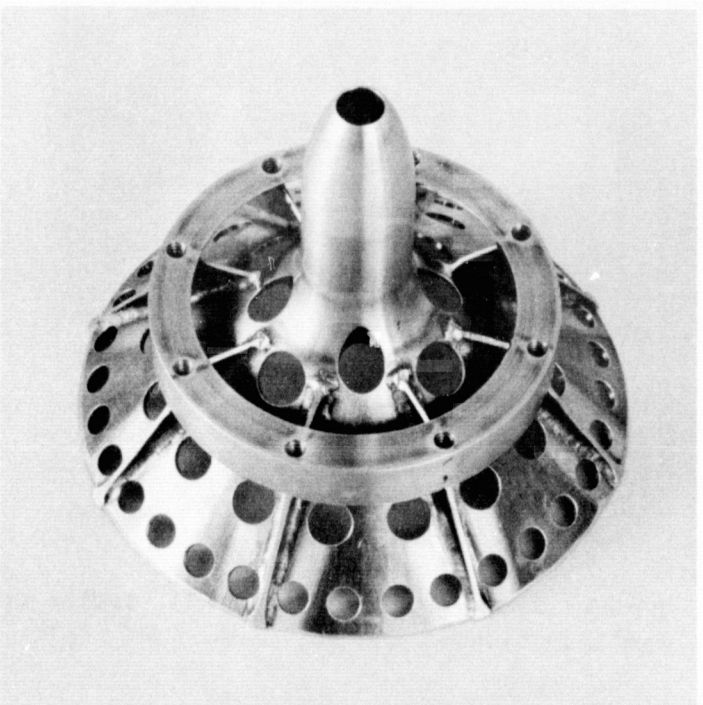

Fig. 8. Flameholder R1, configurations BL, C, BC, and CH

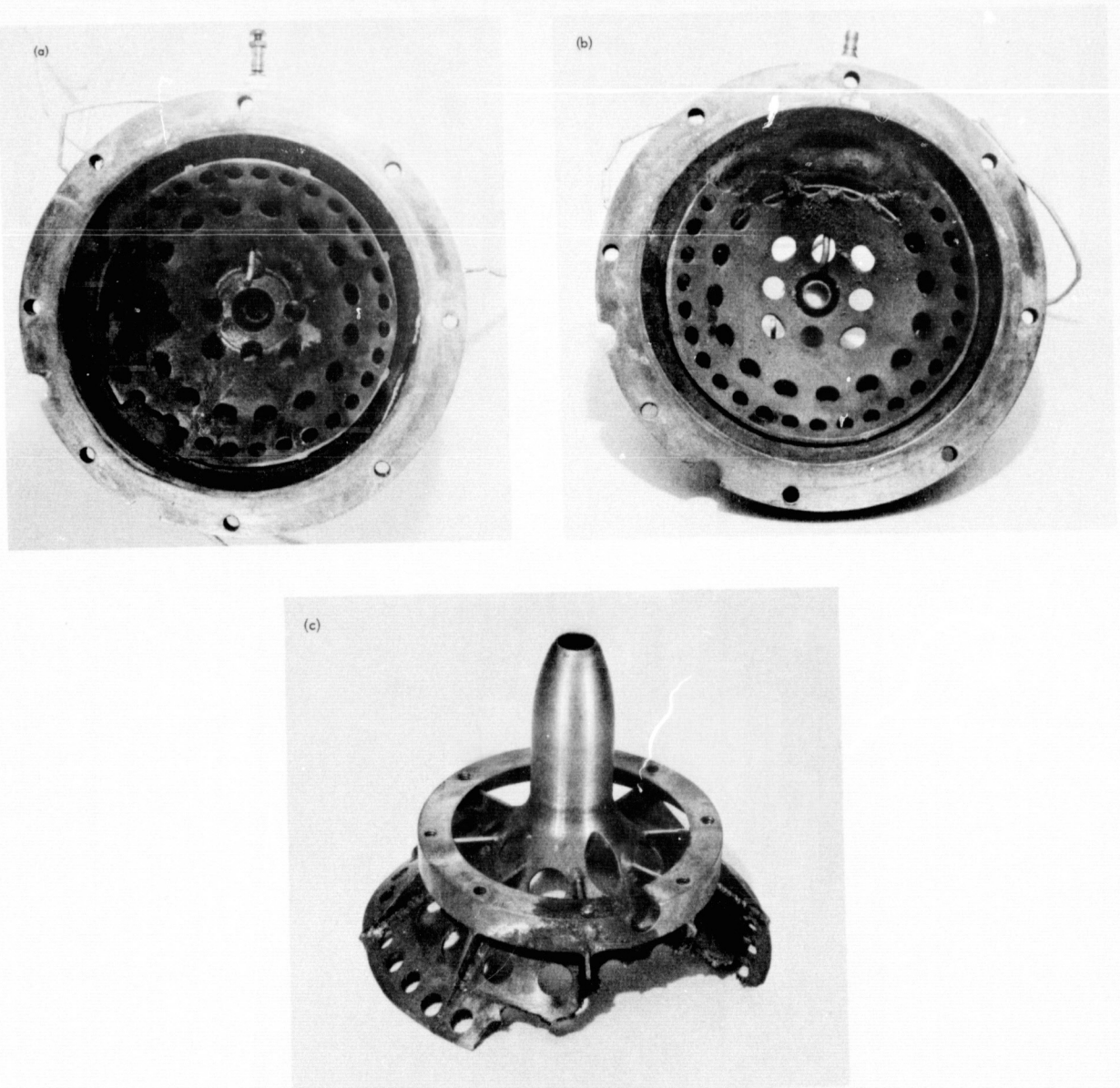

Fig. 9. Typical damage to flameholder R1, cruise condition, configurations C and BC

Even with the ignitor relocated, complete failure of the flameholder occurred in the final three high-power runs after being at condition for periods of about 20 minutes. These failures occurred suddenly and little was left of the flameholder except the mounting rings which were undamaged thermally. Remnants of the welded support web attachments after the second and third runs suggested cracking and fatigue stress, however, and so the final run was made with a further mounting modifications as shown in Fig. 10a. For this version, designated R3, the support webs were doubled in thickness and left free-floating in the mounting ring. During this run, the failure occurred as the H_2 feed system was being purged and it is suspected that a momentarily high H_2 flow may have occurred. In any event, remnants of the supporting webs showed extreme heat stress along the weld joints, which suggests that flame occurred on the upstream surface of the flameholder although upstream mixture temperature was normal to the time of failure.

Figure 10 also shows the flow area modification made for the final two runs for which a new dome and inlet spool were used. With these new components, the need for the extended nose piece was eliminated. For the version shown in Fig. 10b, designated R2, the apex flow area was increased further. For the final version (R3, Fig. 10a), the central flow area was the same as for R1, but the skirt perforations were eliminated in a further attempt to shift the recirculation region downstream from the apex region. This increased the total blockage to 86% for R3.

All of the atomizer/premix/flameholder combinations and their associated runs are summarized in Table 3 where an overall configuration designation is given. This overall designation will be referred to in later sections.

B. EXPERIMENTAL PROCEDURE

The emissions data were obtained during runs of 1 to 3 h duration with constant inlet air conditions corresponding approximately to the selected simulated power level (see Table 4). The burner was operated with jet fuel only and with H_2/jet-fuel mixes over a range of input equivalence ratio, generally from a high of about 0.6 to a low just above total lean blowout. The latter was observed operationally as complete loss of flame. Because of the constant-area exhaust nozzle, it was necessary to modulate the air mass flow rate as equivalence ratio was varied in order to maintain a nearly constant inlet air pressure in the plenum.

All experimental data were digitally recorded on magnetic tape and subsequently reduced by computer. Each data point was obtained with flow conditions held constant until gas analysis, which was continuously monitored, indicated steady values.

For the low and cruise power experiments, ignition was established with jet fuel only at the nominal air flow conditions for the power level. Ignition usually occurred smoothly at an input equivalence ratio of 0.7-0.8. For the takeoff power runs, ignition was generally established near the low power level of air flow but with an elevated air temperature. Operation at an equivalence ratio of about 0.6 was then maintained by increasing jet fuel flow as air flow and air temperature were gradually increased to the nominal takeoff power condition. Approximately an hour was required to accomplish this.

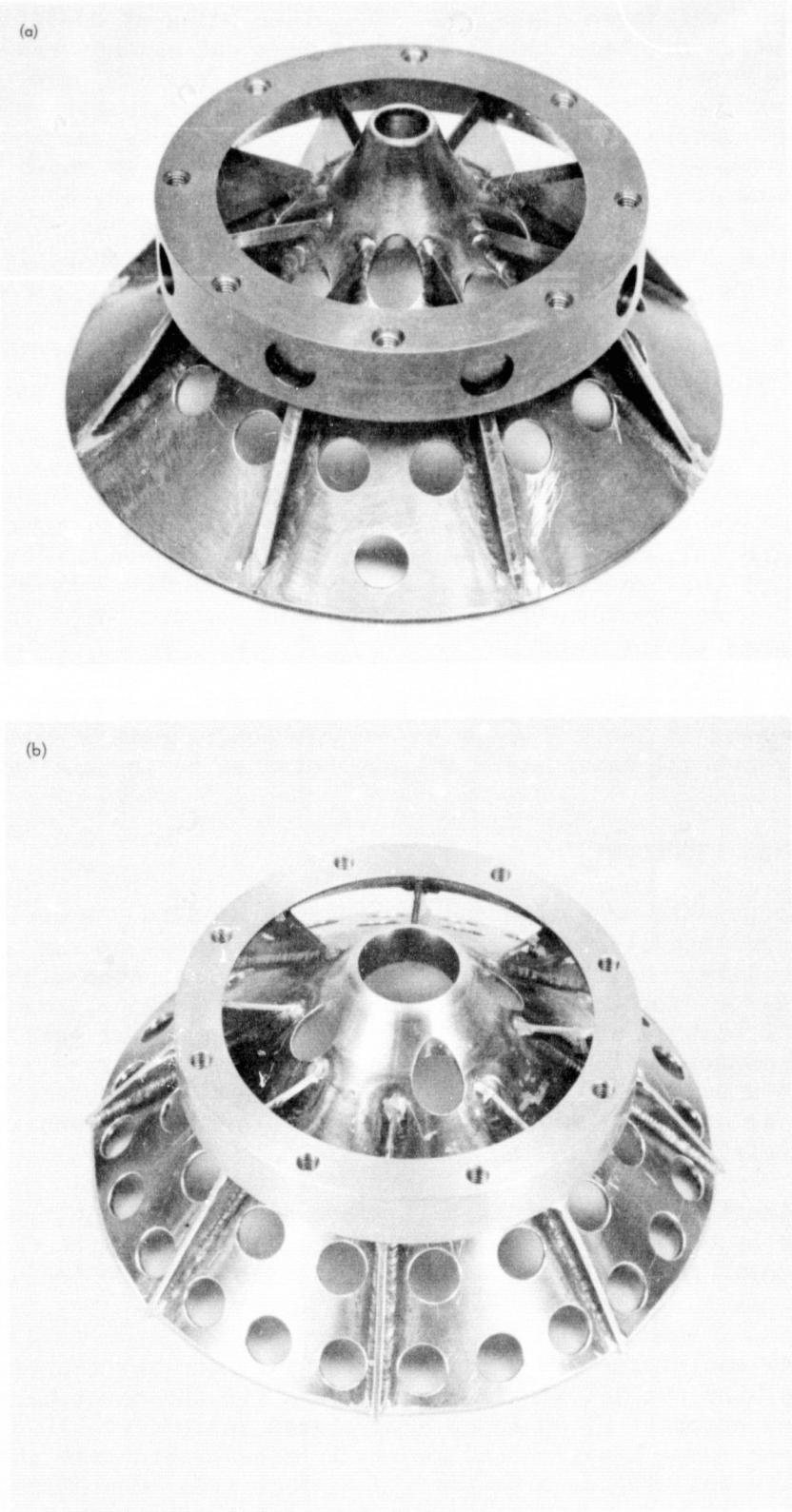

Fig. 10. Flameholder versions for final takeoff power runs

C. COMBUSTION GAS SAMPLE PROBE AND SAMPLE ANALYSIS

On-line analysis of combustion gas composition was accomplished by means of a water-cooled probe, an electrically heated sample transfer line, and a so-called emission analysis bench. Gas samples were analyzed on a dry volumetric basis for O_2, CO_2, NO_x, CO, and unburned HC.

The water-cooled probe (Fig. 11a) was mounted through the exhaust nozzle, as shown in Figs. 1 and 11b, on the centerline axis of the burner assembly, with the probe entrance located a fixed 36.8 cm (14.5 in.) from the flameholder skirt and in the subsonic approach flow to the nozzle sonic plane. Cooling provided by annular water passages was such that the gas sample stream temperature never exceeded 480 K (404°F) 1.2 m (4 ft) downstream of the probe entrance. The gas sample passage surface was stainless steel, plated with a gold film to discourage wall catalysis effects on NO_x. Passage diameter was a constant 0.79 cm (.31 in.) throughout.

The total sample from the probe was transferred to the emission bench location via heavy-walled, stainless steel tubing about 91 m (300 ft) long, through the walls of which a low-voltage ac electrical current was passed to maintain approximately 423 K (302°F) wall temperature. The inside diameter of the transfer line was essentially the same as for the probe. The line was vented to atmosphere at the emission bench location after a small portion of the gas sample was withdrawn by the emission bench pumps. The total gas transferred was of the order of 1/2% of the combustor flow, which resulted in a transit time of 2 s or less to the emission bench.

Gas analysis was conducted using chemiluminescence, FID, and NDIR instruments for NO_x, HC, and CO and CO_2, respectively. A paramagnetic instrument was used for O_2 concentration analysis.

III. RESULTS AND DISCUSSION

Emission results are presented separately for the three different simulated power conditions in terms of variables calculated from input (metered) flow rates. In this presentation Emission Index (EI) is the dependent variable with units of grams of pollutant species per kilogram of total fuel (H_2 + jet fuel). Equivalence Ratio (ER) is used as the independent variable and is based on the stoichiometry of the particular H_2/jet-fuel/air mixture. Mass-percent H_2 in the total fuel is presented parametrically. Except for a few cases that will be noted for the low power condition, atomizer N_2 flow was nearly constant for all data at 4 to 5% of the air mass flowrate. Pertinent calculation procedures are described in Appendix C.

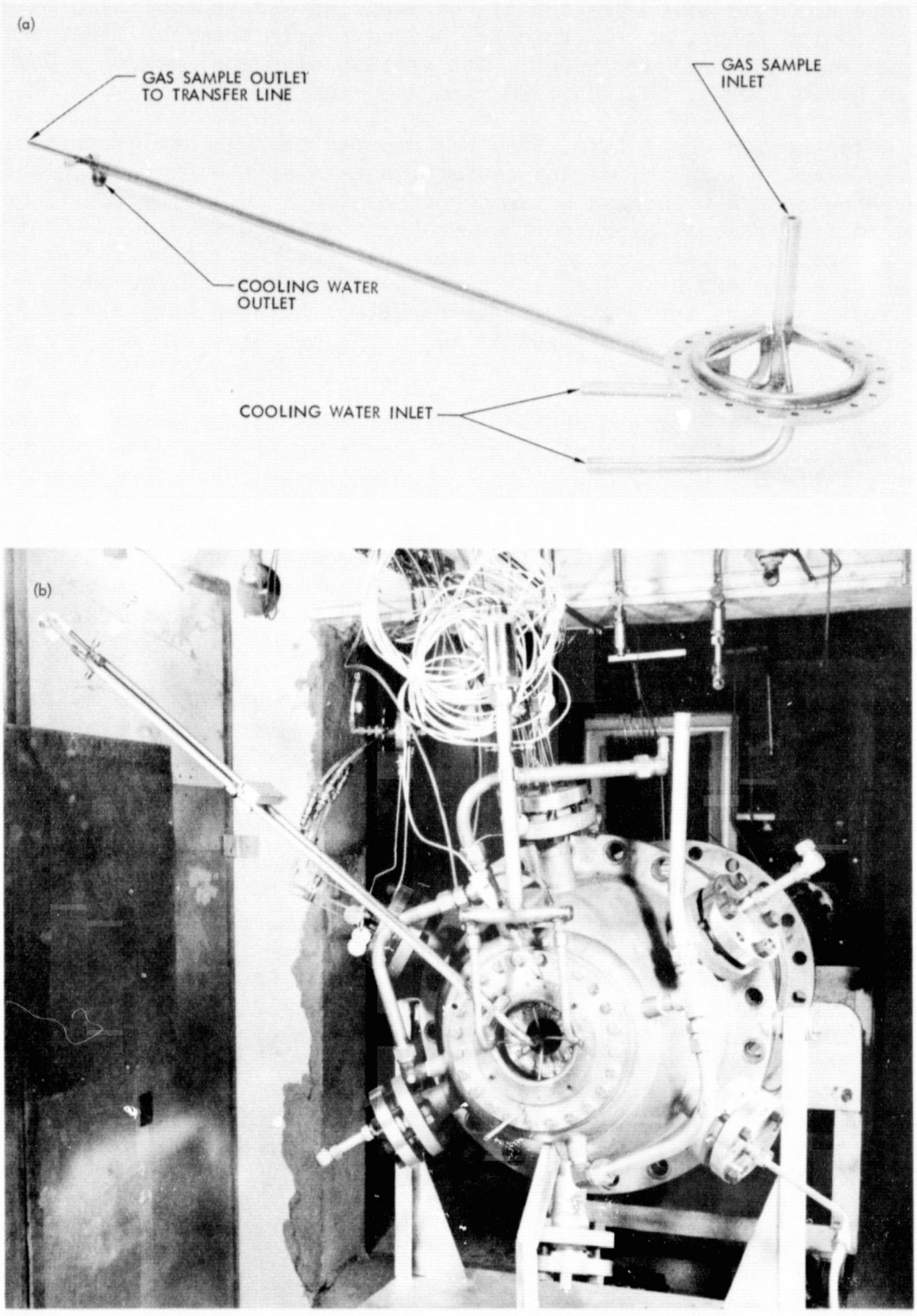

Fig. 11. Gas sample probe and installation

A. LOW POWER CONDITION

Emissions results for overall burner configurations AL, BL, and C (see Table 3) are summarized in Figs. 12, 13, and 14, respectively. The solid-line curves represent the trends for jet fuel only operation (open symbols). The broken lines (solid symbols) show the trends with H_2/jet-fuel mixes. The numbers beside the solid symbols indicate mass-percent H_2. Lines of constant H_2 percentage have not been constructed since the observed data scatter seems to preclude this as meaningful.

All three variants of the burner showed a marked increase in HC and CO as ER was increased from near the lean-blowout (LBO) value for jet fuel only (ER $\sim$ 0.37). This trend was followed whether H_2 was used or not and will be seen to be contrary to the trends for the higher power conditions.

Configuration AL was tested over the widest range of ER and it is clear from Fig. 12 that the use of H_2 permitted leaner burner operation than was possible with jet fuel only. This configuration was also operated for a few minutes with H_2 only at an ER of 0.17, with LBO occurring at 0.16. No emissions data were obtained for that operation, however.

The leanest ER for which emissions data were obtained was 0.303, using 36% H_2, where EIs of 0.41, 10.0, and 0.75 were noted for NO_x, CO, and HC, respectively. Study of Fig. 12 will show a range of ER between 0.3 and 0.4 where two of the three EIs would meet the target level, but no point where all three levels were met simultaneously. This was governed by the tradeoff between NO_x and CO.

Several jet-fuel-only data points are identified with flags in Fig. 12 at higher ER. These data were obtained with atomizer N_2 flow increased to about 6% and improved atomization or mixing reduced CO markedly at the higher jet-fuel flow rates. A smaller reduction in HC was noted.

The data for configuration BL (Fig. 13) show that all the emissions were adversely affected by the changes to the mixing section and flameholder associated with this configuration. The sharper rise in HC and CO with increasing ER suggest the result of decreasing the recirculation region in the apex of the flameholder by opening the flow area there. The generally increased level of all emissions for mixed fuels suggests that H_2 mixing was impaired rather than improved by the mixing section changes.

Configuration C was perhaps the best of the three variants at lean ER, but an impending flameholder failure precluded mixed-fuel operation at an

ER below 0.45. The sharp rise in CO and HC (Fig. 14) with increasing ER was similar to that for the BL configuration, and indeed the same R1 design flameholder was used. The trends of the emissions for mixed-fuels operation were similar to those for configuration AL, and this is consistent with returning to the same (standard) mixing section. The substitution of the cruise power atomizer head was intended to improve the fuel distribution, and the lowered minimum HC levels perhaps reflect that the jet-fuel distribution was improved; however, as will be discussed later, it is doubtful that the H_2 distribution was improved.

Comparison of the NO_x emissions with kinetic-limited estimates (which are described below) shows that all variations of the burner yielded NO_x concentrations about three orders of magnitude too high at the leanest operating point. Similarly, the CO concentrations were much higher than equilibrium levels.

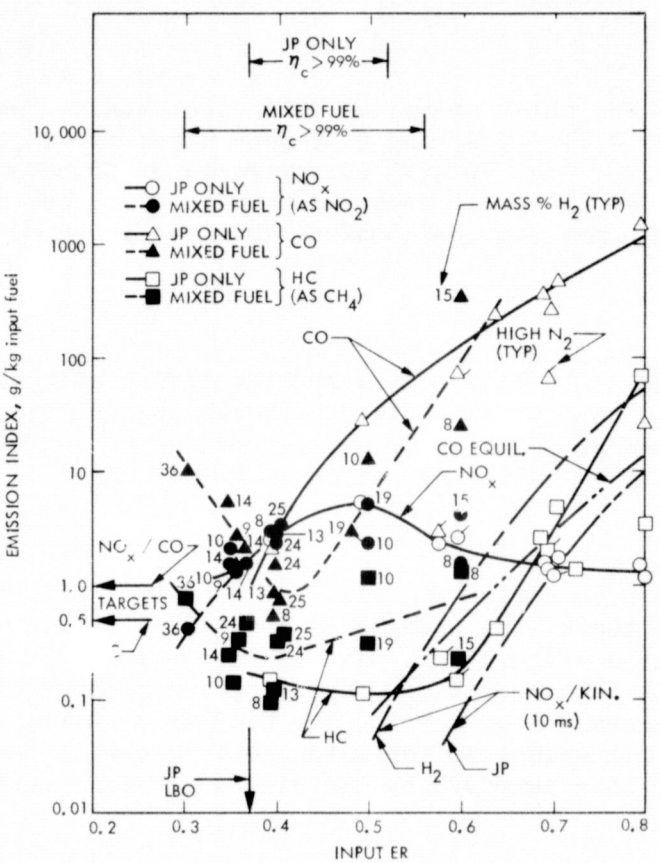

Fig. 12. Low power emissions, configuration AL

ER below 0.45. The sharp rise in CO and HC (Fig. 14) with increasing ER was similar to that for the BL configuration, and indeed the same R1 design flameholder was used. The trends of the emissions for mixed-fuels operation were similar to those for configuration AL, and this is consistent with returning to the same (standard) mixing section. The substitution of the cruise power atomizer head was intended to improve the fuel distribution, and the lowered minimum HC levels perhaps reflect that the jet-fuel distribution was improved; however, as will be discussed later, it is doubtful that the H_2 distribution was improved.

Comparison of the NO_x emissions with kinetic-limited estimates (which are described below) shows that all variations of the burner yielded NO_x concentrations about three orders of magnitude too high at the leanest operating point. Similarly, the CO concentrations were much higher than equilibrium levels.

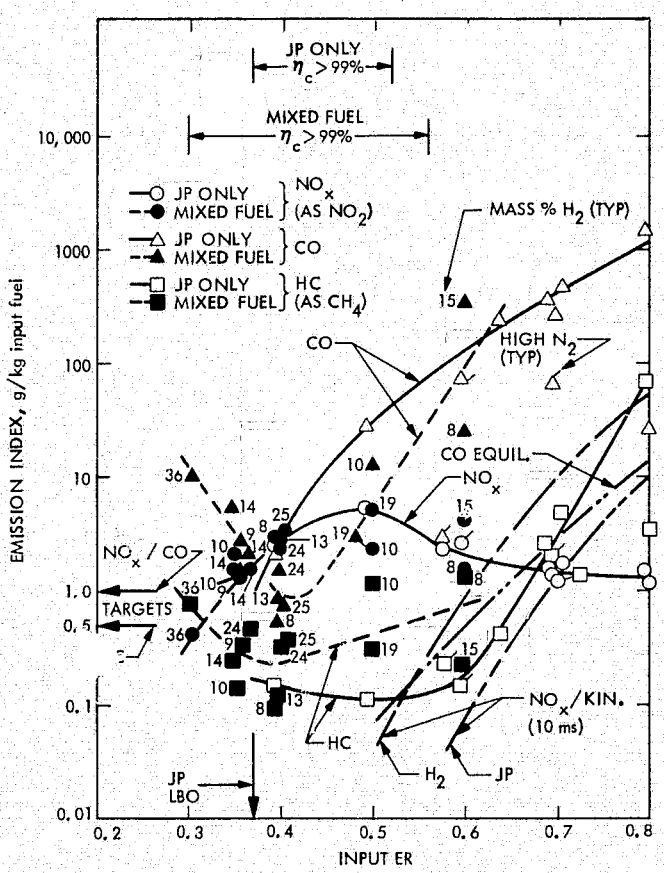

Fig. 12. Low power emissions, configuration AL

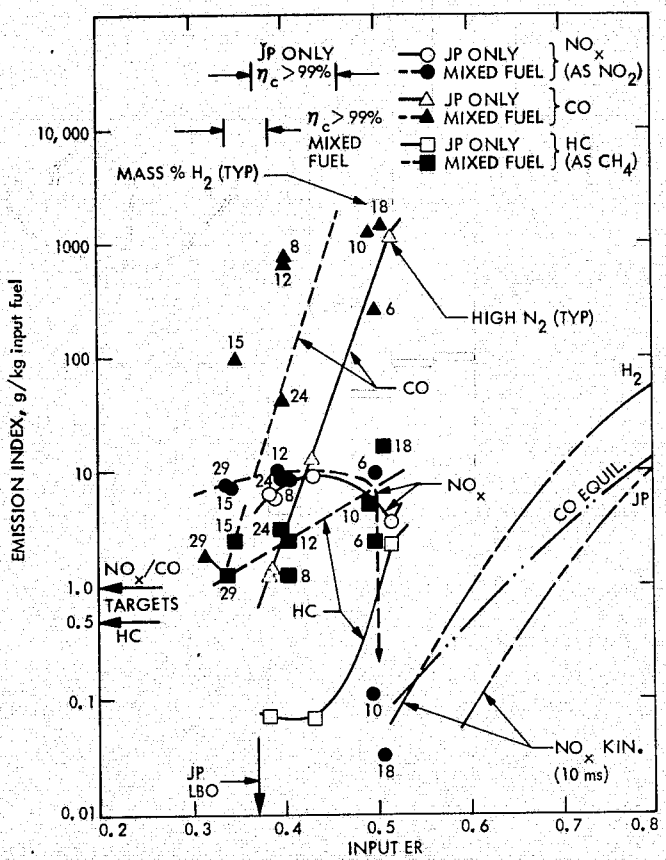

Fig. 13. Low power emissions, configuration BL

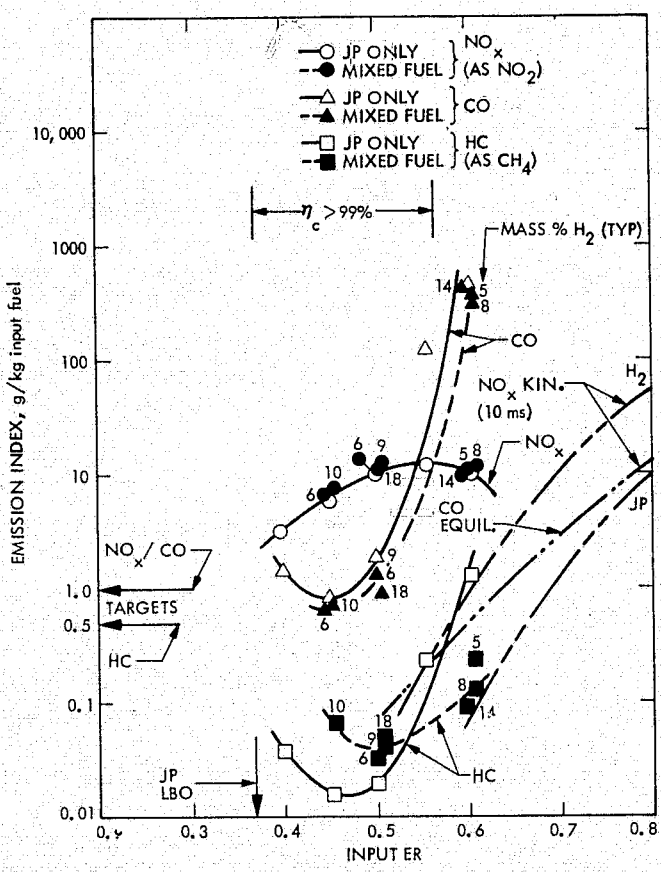

Fig. 14. Low power emissions, configuration C

B. CRUISE POWER CONDITION

Cruise condition results are presented in Figs. 15, 16, and 17 for CO, HC, and NO_x, respectively. Data for each burner configuration are shown on each figure. This different format is used for the cruise results since there is no significant difference in the CO and HC emission trends for the three burner variations, and the beneficial effects of H_2-enrichment on lean limit extension can be more clearly illustrated. As was done for the low power results, the solid curves and open symbols represent data for jet-fuel-only operation while the broken curves and solid symbols are for mixed-fuels operation.

When the burner was operated with jet fuel only, equilibrium or lower levels of CO (Fig. 15) and very low levels of HC (Fig. 16) were observed for input ERs from 0.7 down to a little under 0.55, where both emissions increased rapidly with further decrease in ER. At an ER of about 0.53, a nearly discontinuous change to the sample gas composition occurred, which was most obvious in O_2 and CO_2 measurements. This change was ultimately interpreted as a partial blowout of the combustion process behind the flameholder, and this behavior is indicated as such in Figs. 15 and 16. This transition was not apparent while operating the burner; indeed total LBO was not observed until an ER of 0.37. Data for CO and HC in the transition region between partial and total LBO are identified with crosses in the open symbols. The interpretation of a partial blowout will be further substantiated in Section IV.

The dashed curves in Figs. 15 and 16 are constructed through data for 10-12% input H_2 in the total fuel. For clarity, those data are not numerically identified, but data for H_2 concentrations falling outside of this range are marked as before. Operation with mixed fuels eliminated the indication of partial blowout as deduced from O_2 and CO_2 measurements, and clearly, the presence of H_2 provided a lower total LBO which, for 14% H_2, was observed at ER = 0.26. The improvement in flame stability with 10-12% H_2 permitted operation of the burner down to an input ER of 0.38 before the CO emission index target of 1.0 g/kg fuel was exceeded, and at that ER, a HC level of 0.1 g/kg fuel is still well below the target value of 0.5.

The premixed flame model and calculation procedures of Westenberg (Ref. 17) were used to estimate kinetically-limited CO oxidation for lean combustion at a constant 10 ms dwell time. The results of these calculations are shown in Fig. 15 for jet fuel only and for mixed fuels at a constant air-to-H_2 mass ratio of 350. The effect of atomizer N_2 on reducing flame temperature was accounted for. The proportion of H_2 in the total fuel varies continuously along the latter kinetic curve as illustrated in Appendix A, Fig. A-1, and three levels of H_2-enrichment are identified on the mixed-fuel curve in Fig. 15. These are near the input H_2 concentrations used in the experiments. For simplicity, the kinetic curves are shown to intercept the equilibrium CO curve, but actually they approach the equilibrium line asymptotically in the fuel-rich direction. Also, the equilibrium curve is for jet fuel only (with atomizer N_2), as are all the equilibrium CO results presented in this report. This is acceptable because, when evaluated as a function of combined input ER and for the relatively low H_2 concentrations of interest here, equilibrium CO changes only slightly for the mixed fuel.

Comparison of the experimental and calculated results shows that mixed-fuel operation yielded CO emissions approaching the kinetic estimates, which is in significant contrast to the results for jet-fuel-only operation. It is acknowledged that improvement in flame stabilization technique might improve lean-burning performance for jet-fuel-only operation, but then mixed-fuel performance would also undoubtedly be improved. Thus, the feasibility of using mixed fuels to achieve a substantially depressed lean operating limit in order to maintain ultralow CO (and HC) emissions is well demonstrated in these cruise power results.

Contrary to the HC and CO results, NO_x emissions levels did change for the different burner variations as shown in Fig. 17. This was especially true for variant BC, for which NO_x levels were higher. No mixed-fuels data were obtained for configuration AC because of the excessively limited durability of the hub-mounted flameholder. The open symbols with crosses again represent data for ERs between partial and total LBO.

In Fig. 17, the experimental NO_x results are compared to calculated results based on chemical kinetics for 100% jet fuel and 100% H_2, assuming one-dimensional flow for a constant 10 ms dwell time. For the NO_x calculations, atomizer N_2 was not included; therefore full flame temperature was assumed. A computer program (Ref. 18) was used to numerically integrate the rate equations for a set of eight elementary reversible reactions (including the principal Zeldovich reactions) generally accepted as important rate controlling steps for post-flame production of oxides of nitrogen (cf. Ref. 6). The possibility of "prompt NO" was arbitrarily neglected since its importance under lean conditions is likely to be small. These kinetic estimates probably cannot be considered as "predictions" for the complex recirculation region produced by the flameholder, but they do serve as a reference for one limit of NO_x production.

Jet-fuel-only operation produced NO_x trends which approximate classical exponential dependency on ER, but with magnitudes greater than the kinetics estimates. For a fixed input ER, introduction of H_2 further increased the NO_x emission. This was expected because, at a fixed ER, flame temperature increases with H_2 concentration in the total fuel. The kinetics estimates for 100% H_2 and 100% jet fuel in Fig. 17 show this. However, the increases observed in these experiments are much greater than the kinetics estimates suggest. Nonetheless, configuration C yielded the target NO_x emission index of 1.0 g/kg fuel at an ER of 0.38 using 10-12% H_2.

Thus, configuration C exhibited an operating point for the cruise condition which satisfied all the target emissions simultaneously, although without the margin believed to be attainable with respect to NO_x. It is further observed that such an operating point was not achievable with jet fuel only, owing to excessive CO and HC at ER low enough to reduce NO_x to the target level.

It is finally observed that a premixed primary zone ER of 0.38 at least approaches a feasible cruise design condition for the burner of an operating gas turbine engine of the 30:1 compression ratio class, where, typically, an overall ER of 0.31 is required for cruise power. A premixed heat release zone of 0.38 would leave about 20% of the total air flow for cooling and dilution. Cooling requirements should be much reduced from current practice due to the ultralean (cooler) burning zone. This cruise condition operating point is also discussed in Appendix A relative to the overall H_2-enrichment concept.

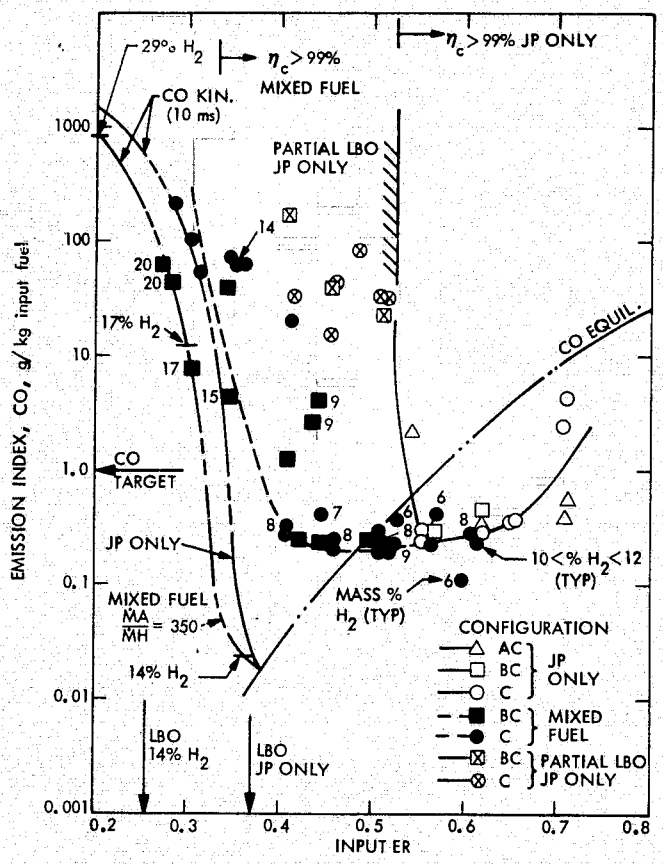

Fig. 15. Cruise power CO emissions, configurations AC, BC, and C

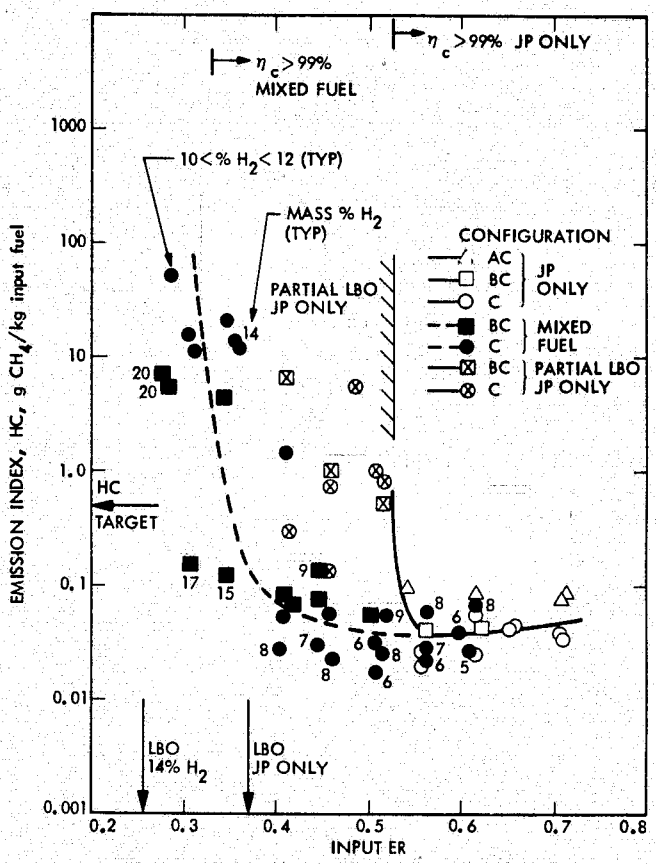

Fig. 16. Cruise power HC emissions, configurations AC, BC, and C

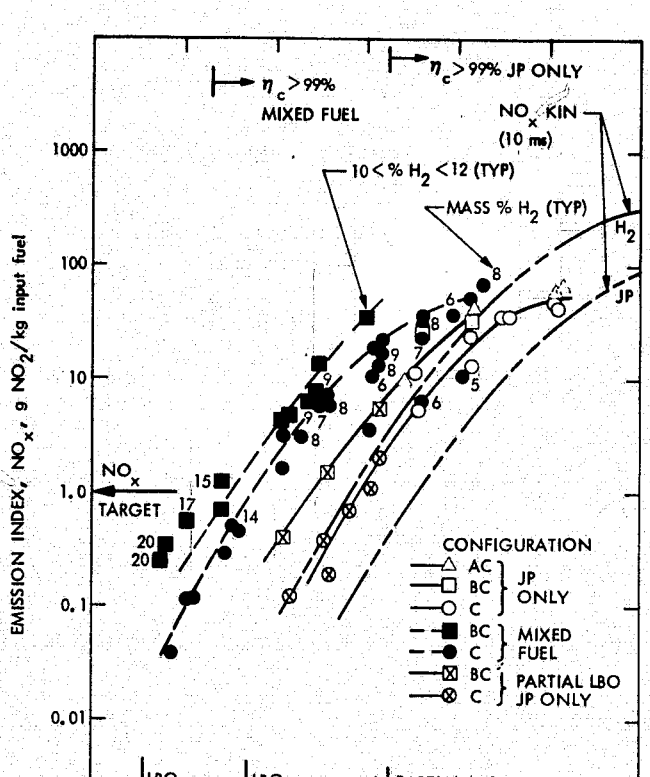

Fig. 17. Cruise power NO_x emissions, configurations AC, BC, and C

C. TAKEOFF POWER CONDITION

Emission results for the simulated takeoff condition are shown in Fig. 18 for burner configurations CH, D, and E. No data for mixed-fuel operation was obtained as previously discussed. The greatest range of data was obtained for configuration CH which produced excessive levels of CO below an ER of 0.5, although HC emissions remained at an EI of 0.1 or less to the lowest ER of 0.41. The NO_x emissions followed the slope of the kinetics estimates but again were of substantially greater magnitude.

The limited range of data for configurations D and E restrict comparison of emissions to ERs in the range of 0.55 to 0.6, where somewhat lower levels of all emissions were measured relative to configuration CH.

Although it was not demonstrated, it is doubtful that any of these variations to the Mod 2 burner would have yielded target No_x emission levels with

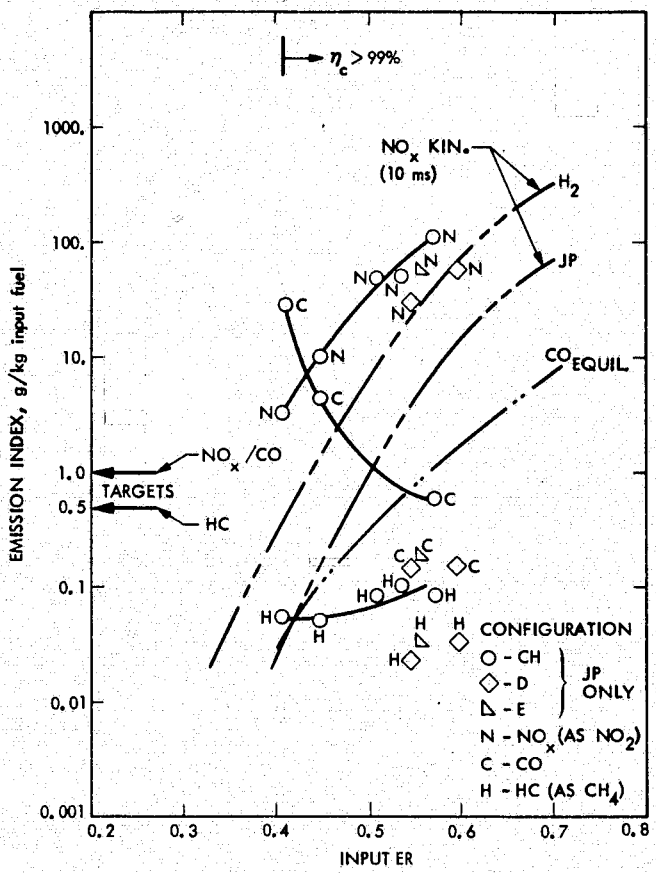

Fig. 18. Takeoff power emissions, configurations CH, D, and E

mixed-fuel operation at takeoff conditions. Taking the 20% allowance for cooling and dilution air mentioned for the cruise condition and a typical engine power requirement for an overall ER of 0.34 gives a minimum allowable premix ER of 0.43. Comparison of the jet-fuel-only data for NO_x at takeoff conditions (Fig. 18) with the NO_x data for the cruise condition with and without H_2 (Fig. 17), reveals the improbability of achieving 1.0 g NO_x/kg fuel at that input ER with the present Mod 2 burner.

D. PRESSURE LOSS (ALL CONDITIONS)

Total pressure loss from plenum to combustor exit (end of cylindrical chamber) was measured throughout the range of these experiments and was observed to vary with ER and flameholder version. The total range observed was from 4% to 8% of plenum pressure. For overall configuration C, the pressure loss was 7% at ER = 0.38 at the cruise power condition. The quoted pressure losses include the losses at the bell mouth entry to the mixing section.

IV. ANALYSIS OF CRUISE RESULTS

Although the results for the cruise power condition showed that the ultralow target emissions were simultaneously achieved at a useful input ER for the C configuration of the burner, the margin of achievement of the NO_x target appears to be much lower than the kinetics estimates suggest as possible. The relatively poorer characteristics for all emissions at low power and excessive NO_x at high power further indicate that nonoptimized performance was realized.

Moreover, the persistent problem with flameholder durability appeared to have occurred in a peculiar way since the severity of the problem consistently increased as the input ER was reduced to very lean values with H_2-enrichment. This result is seemingly contrary to the expected reduced heat loads that would go with reduced flame temperature and burning rates for the leaner mixtures.

In view of these observations, it is instructive to examine the measured gas sample compositions with the objective of establishing whether a consistent indication of nonuniform premixing was present in the data. In particular, the view will be taken that the gas sample extracted through the single-point probe could be heavily biased by the combustion gas flow near the axial centerline of the combustion chamber, and further, that this flow could reflect to a large degree the burned gas composition from the apex region of the flameholder. This is an important region since the variations in the flameholder flow area there were observed to produce variations in emissions, flameholder durability, and ignition/stability characteristics.

To that end, the sample gas compositions for cruise configuration AC and C were used because the most complete O_2 and CO_2 data were obtained during those runs. Using standard chemical balance arguments (described in Appendix C), jet-fuel ER, H_2 ER, combined ER, and mass % H_2 were evaluated for each data point from the measured volumetric concentrations of O_2, CO_2, CO, HC, and NO_x. The N_2 concentration was not measured; therefore, atomizer N_2 was assumed to be distributed uniformly with the jet fuel. Spot checks of the effect of assuming that the N_2 was uniformly distributed with the air revealed no significant differences in the trends of the results.

Results of these calculations expressed as a ratio of the sample-to-input ER for the respective fuels versus the combined input ER are shown in Fig. 19. The solid symbols are for mixed fuels and the open symbols are for jet-fuel-only operation. The analogous ratio for the combined sample ER (data not shown on Fig. 19) was found to be essentially constant at 1.3 over the entire range of input ER.

Excellent agreement was obtained in comparing the measured O_2 and CO_2 concentrations with expected equilibrium values for the combined ER calculated from the gas samples, except for the data on Fig. 19 marked with crosses. As can be seen, these data also do not follow the mean trend of the results for jet-fuel ER. After a review of the experimental measurements for those data failed to reveal any discrepancies in the flow and gas analysis measurements, it was concluded that the most reasonable interpretation was that the probe and/or sample transfer line had not delivered a sample with the true HC content to the gas analysis instruments. The cause of this has not been fully resolved but there is reason to believe that with very large concen-

trations of HC considerable condensation, particularly of the heavier HC fractions, can occur under the high pressure at the inlet end of the transfer line. This argument is consistent with HC saturation limits for the measured state conditions at the inlet, assuming a HC mass concentration of the order of 3% that would be present for blowout. If this occurs, the liquid can collect at bends and fittings or be blown out the vent end of the line, but in either case the HC content of the true sample will not be accurately detected by the analytical instruments.

With the assumption that the true jet-fuel ER for these anomalous data should approximately follow the mean trend of the bulk of the data, the hydrocarbon levels were adjusted upward to satisfy the carbon balance dictated by the CO and CO_2 measurements. These computations yielded combustion efficiencies in the range of 50-60% and ERs for which the measured O_2 and CO_2 concentrations were off-equilibrium in the appropriate directions (high O_2 and low CO_2) for incomplete combustion.

Thus, the crossed data points are believed to reflect erroneously low measured HC levels and are interpreted as indicating a partial blowout in the central region of the combustor. Previous reference was made of this operating mode in Section III (Figs. 15, 16, and 17).

Further examination of the calculated results shown in Fig. 19 at once reveals that the input H_2 is probably very poorly distributed behind the flameholder, with excessive concentration in the central region. This maldistribution appears to worsen as the burner is leaned. Distribution of the jet fuel is apparently much better than for the H_2, with the single point characterization implying uniformity for input ER = 0.46. But, interestingly, the jet fuel tends to shift spatially in the opposite direction from the H_2 as the combined input ER is leaned, as if the H_2 were displacing the jet fuel. To lend perspective to these ER ratios, the overall range of sample ERs associated with the mixed-fuel distributions are 0.15 to 0.35 for the H_2 and 0.17 to 0.62 for the jet fuel.

The combined effects of the distribution variations on H_2 concentration in the total fuel near the central region is shown in Fig. 20. The lower plot shows the ratio of sample-to-input H_2 concentration versus combined input ER. This is translated to absolute values in the upper portion of Fig. 20, where the entire range of the data are enclosed within the envelopes shown. Possibly, nearly 50% H_2-enrichment was present (locally) at the leanest input ER, with about 30% at input ER = 0.38, where the target emissions were achieved. This input ER corresponds to a combined sample ER of about 0.5 as deduced from the gas sample.

The unmixedness indicated by these results is qualitatively consistent with the results from the ancillary mixing tests conducted before the combustion experiments, where the tendency for high H_2 concentration near the center of the mixing section was previously noted. Moreover, the overall richness of the central combustion region is consistent with the greater-than-expected NO_x emissions. Finally, the excessive H_2-concentration in the apex region of the flameholder and its increasing trend with lean input mixtures could explain the observed adverse effect of lean operation on the flameholder, where the relatively fast burning rate for H_2 may, in fact, have increased the heat load to the downstream surface of the flameholder.

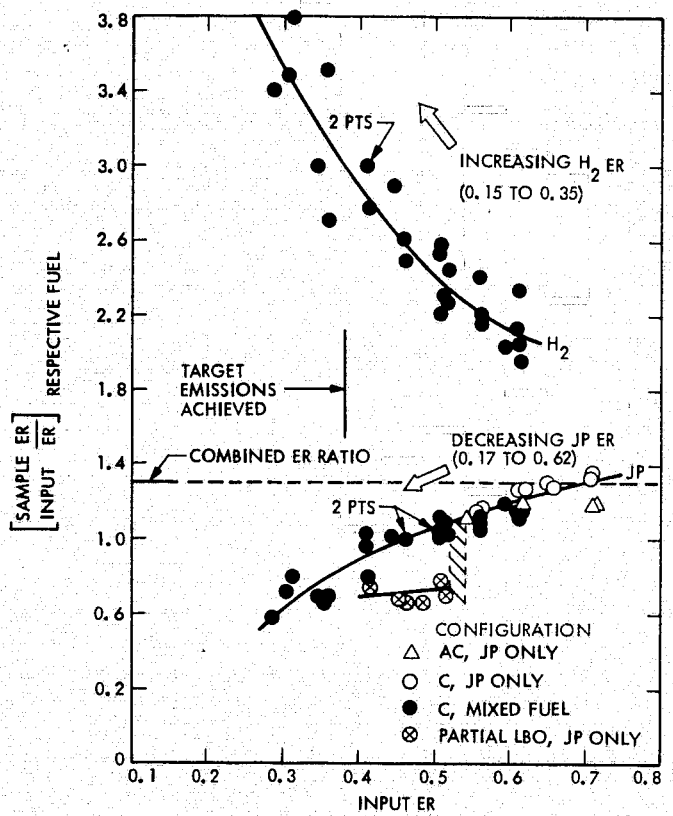

Fig. 19. Cruise power, ratio of sampled to input equivalence ratio

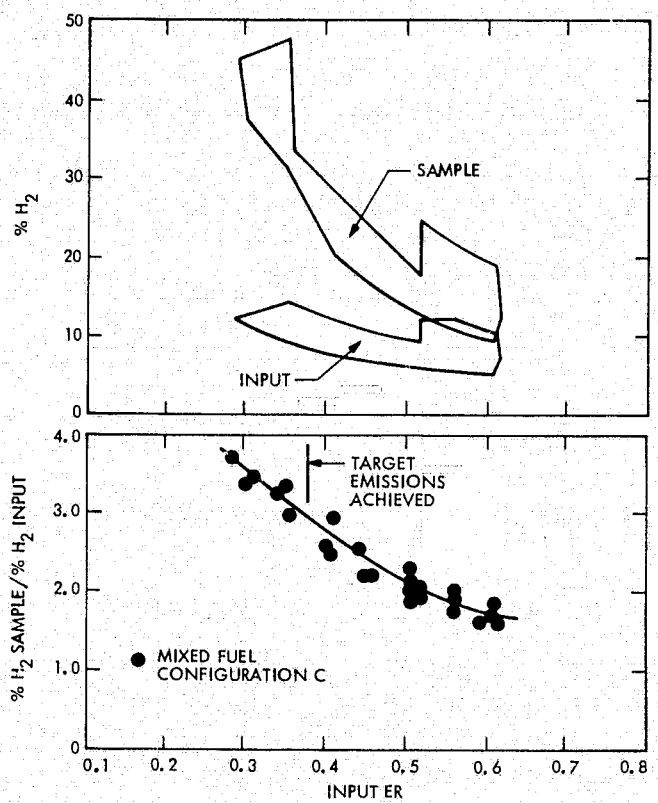

Fig. 20. Cruise power, comparison of sampled to input H_2 mass concentration

It could be argued that the high H_2 concentration should have suppressed the increase of HC and CO emissions to leaner ERs than were observed, that being the justification for using H_2-enrichment. But application of the concept implies homogeneous mixing of the H_2/jet-fuel/air. In the event that small-scale nonuniformity existed locally (such as incomplete jet-fuel evaporation) the tendency for incomplete HC combustion might still surface with ultralean burning (low temperatures), even with high H_2 concentration. For example, if the H_2 is considered to burn independently of the jet fuel, its contribution to flame temperature is only 1550 K (2330°F) at the maximum H_2 ER of 0.35 deduced from the sample gas (Fig. 19). As poor as the mixing may have been, however, the very beneficial effects of the H_2 on the combustion of the HC are emphasized in Fig. 21.

Figure 21 shows the HC and CO EIs based on the jet-fuel ER as inferred from the sample composition. The significance of these results is that for this fixed burner design the use of H_2 has extended efficient HC combustion (99% or better) from a JP ER of about 0.6 where partial blowout was observed down to about 0.2. Jet-fuel ER = 0.3 corresponds approximately to the condition where the target emissions were achieved.

Carrying these results from the sample composition analysis one step further, it can be shown that the seemingly high NO_x emissions (previously noted in Section III (Fig. 17) when NO_x was presented as a function of combined input of combined input ER) are very much closer to kinetic estimates when portrayed as a function of combined sample ER. Moreover, if the combined sample ER for mixed-fuel data is converted to an equivalent JP ER to yield similar combustion temperature, the NO_x emissions for mixed-fuel and jet-fuel-only operation can be compared on a common basis. This conversion was done as shown in Appendix C assuming constant heat capacity and heats of combustion of 1.196×10^8 J/kg (51,571 BTU/lbm) and 4.267×10^7 J/kg (18,400 BTU/lbm), respectively, for the H_2 and jet fuel.

These results are shown in Fig. 22, where it can be seen that the NO_x EIs fall generally within the band of kinetic estimates for 1.0 to 10.0 ms dwell time with relatively good agreement in the overlap region between mixed-fuel and jet-fuel-only data.

In summary, this analysis of the sample gas results does indeed indicate consistent premixing deficiencies in the experimental burner. And although the analysis was for the cruise power results, qualitatively, the same must also apply to the low and takeoff power conditions. The low inlet temperature associated with the low power condition (nearly idle) adversely affects liquid fuel evaporation; hence, this far off-design operating mode accentuates the difficulty in achieving thorough premixing.

If the sample gas compositions are considered as more representative of the performance of the concept with this burner under cruise conditions, then it can still be stated that the ultralow target emissions were only obtainable with H_2-enrichment and that they were achieved at a burning ER of 0.50 with 30% H_2. This burning ER is still a potentially useful primary zone mixture ratio.

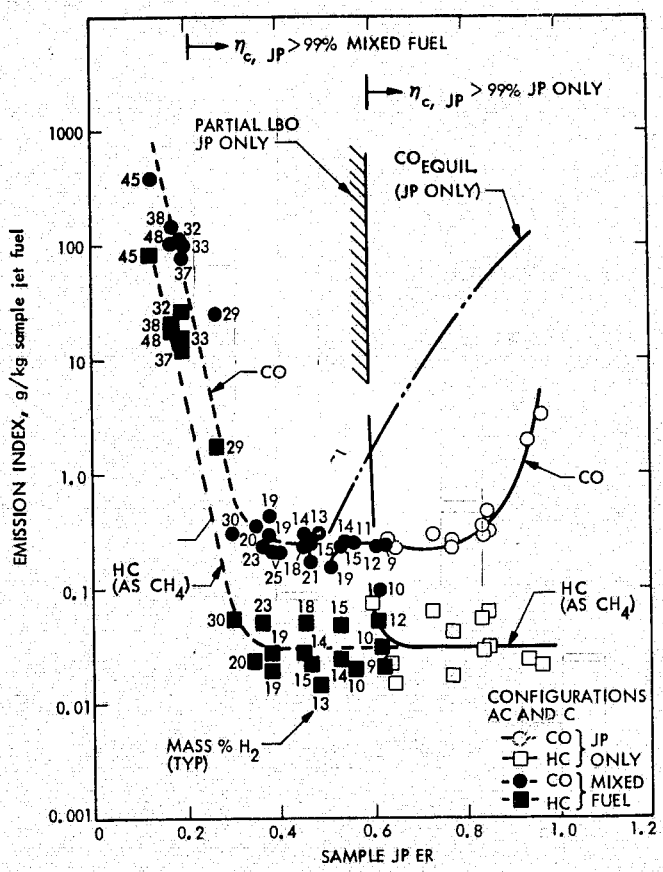

Fig. 21. Cruise power, CO and HC emissions on basis of jet fuel equivalence ratio from sample

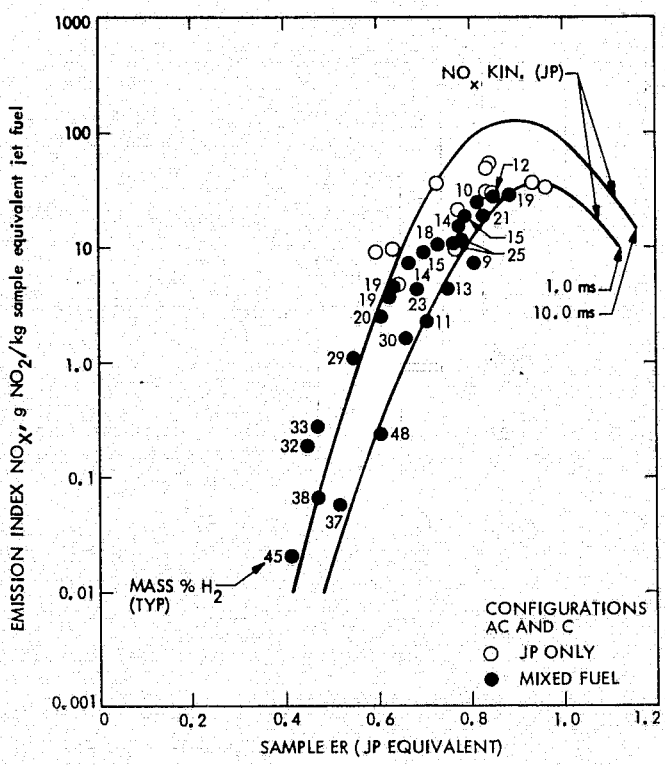

Fig. 22. Cruise power, NO_x emissions on basis of equivalent jet fuel

V. CONCLUSIONS

Conclusions are as follows:

(1) The ultralow target emission levels were simultaneously achieved under simulated cruise power conditions at a burning ER and with pressure losses amenable to practical combustor design. These levels were achievable with the Mod 2 burner with H_2-enrichment, but not with jet fuel only due to the onset of lean blowout at too high an ER to sufficiently reduce the NO_x emission.

(2) The target emissions were not achieved simultaneously at the low power condition because of somewhat excessive CO. However, with H_2-enrichment, a tradeoff between CO and NO_x was possible so that target levels for HC and either CO or NO_x could be achieved. The residual EI for either CO or NO_x was about 3.0 g/kg fuel.

(3) Achievement of the target emission levels at the takeoff power condition with jet fuel only was not possible due to excessive CO and NO_x. Attainment of the target levels with mixed fuels at a usable ER would have been marginal at best for the Mod 2 configurations tested.

(4) Premixing deficiencies, particularly with regard to the H_2, reduced the effectiveness of H_2-enrichment and aggravated the flameholder durability problems in these experiments. Improved premixing should reduce the amount of H_2 required.

(5) As reactant mixedness is improved, the potential of lean burning for minimizing NO_x will be approached, but maintaining flame stabilization and ultralow HC and CO emissions will become limiting practical considerations. Hydrogen enrichment can provide a significant lean-limit extension for minimizing all emissions.

(6) Flame stabilization via a physical flameholder presents a difficult design/development problem due to the exposure of the component to the combustion zone. On the other hand, true achievement of the lowered combustion temperature potentially available with H_2-enrichment should reduce the heat load to the exposed surfaces compared, for example, to present liner environments. Alternate flame stabilization schemes might also alleviate the problem.

(7) Effective implementation of H_2-enrichment is not simple but is feasible with dedicated development. Importantly, the bulk of the premixing problem has to be solved for any lean-burning scheme. Mixed fuels with local compositions to nearly 50% H_2 and with H_2 ER to 0.35 survived the premixing environment imposed by 728 K, 11.75 x 10^5 N/m^2 (11.6 atm) inlet air without preignition or flashback. Extension of these characteristics to higher temperature and pressure remains to be demonstrated, although premixed jet fuel and air exhibited no preignition problem in these experiments up to 30.39 x 10^5 N/m^2 (30 atm) and 800 K.

REFERENCES

1. Osgerby, I. T., "Literature Review of Turbine Combustor Modeling and Emissions," AIAA Journal, Vol. 12, No. 6, pp. 743-754, June 1974.

2. Rudey, R. A., Status of Technological Advancement for Reducing Aircraft Gas Turbine Engine Pollutant Emissions, NASA TMX-71846, Lewis Research Center, Cleveland, Ohio, December 1975.

3. Niedzwiecki, R. W., The Experimental Clean Combustor Program--Description and Status to November 1975, NASA TMX-71849, Lewis Research Center, Cleveland, Ohio, December 1975.

4. Yaffee, M. L., "NASA Seeks Clean Combustors by 1976, "Aviation Week and Space Technology, August 26, 1974.

5. Blazowski, W. S., Walsh, D. E., and Mach, K. D., "Prediction of Aircraft Gas Turbine NO_x Emission Dependence on Engine Operating Parameters and Ambient Conditions," AIAA paper 73-1275 presented at the AIAA/SAE 9th Propulsion Conference, Las Vegas, Nevada, November 5-7, 1973.

6. Blazowski, W. S., "Aircraft Altitude Emissions: Fundamental Concepts and Future R&D Requirements," AIAA paper 75-1017 presented at the AIAA 1975 Aircraft Systems and Technology Meeting, Los Angeles, California, August 4-7, 1975.

7. "Control of Air Pollution for Aircraft Engines--Emission Standards and Test Procedures for Aircraft," Federal Register, Vol. 38, pp. 19088-19103, July 17, 1973.

8. Roffe, G., and Ferri, A., Effect of Premixing on Oxides of Nitrogen in Gas Turbine Combustors, NASA CR-2657, February 1976.

9. Anderson, D., Effects of Equivalence Ratio and Dwell Time on Exhaust Emissions from an Experimental Premixing Prevaporizing Burner, NASA TMX-71592, Lewis Research Center, Cleveland, Ohio, 1975.

10. Rupe, J. H., System for Minimizing Internal Combustion Engine Pollution Emissions, United States Patent 3,906,913, September 23, 1975.

11. Rupe, J. H., "Hydrogen Enrichment of Hydrocarbon Fuels as a Means for Obtaining Low Emissions and High Thermal Efficiency in a Spark Ignition Engine." Unpublished presentation to the Western States Section of the Combustion Institute, October 30, 1973.

12. Hoehn, F. W., Baisley, R. L., and Dowdy, M. W., "Advances in Ultralean Combustion Technology using Hydrogen-Enriched Gasoline," Paper No. 759173 presented at 10th Intersociety Energy Conversion Conference, University of Delaware, Newark, Delaware. August 17-22, 1975.

13. Houseman, J., and Cerini, D., "On-Board Hydrogen Generator for a Partial Hydrogen Injection I.C. Engine," SAE Paper 740600 presented at the 1974 SAE National West Coast Meeting, Anaheim, California, August 12-16, 1974.

14. Menard, W. A., Moynihan, P. I., and Rupe, J. H., "New Potentials for Conventional Aircraft when Powered by Hydrogen-Enriched Gasoline", SAE Paper 760469 presented at the SAE Business Aircraft Meeting, Wichita, Kansas, April 6-9, 1976.

15. Anderson, D. N., Effect of Hydrogen Injection on Stability and Emissions of an Experimental Premixed Prevaporized Propane Burner, NASA TM X-3301, Lewis Research Center, Cleveland, Ohio, October 1975.

16. Clayton, R. M., Initial Results on the Experimental Evaluation of Hydrogen Enrichment for Low Emission Jet Combustors, Unpublished Report to NASA Aeronautical Propulsion Office (Code RL), transmitted by letter dated February 14, 1975.

17. Westenberg, A. A., "Kinetics of NO and CO in Lean, Premixed Hydrocarbon-Air Flames", Combustion Science and Technology, Vol. 4, pp. 59-64, 1971.

18. Laurendeau, N., and Sawyer, R. F., General Reaction Rate Problems: Combined Integration and Steady State Analysis, Report TS-70-14, College of Engineering University of California, Berkeley, California, December 1970.

Table 1. Emission and performance goals and comparison with typical engine

Emission/performance item	Ultralow (JPL) goals[a]	Estimates to meet EPA 1981 LTO cycle[b]	Typical current production engine[c]	Typical best effort emission reduction (burner rig tests)[c]
EI NO_x, g/kg	1.0	13.0 (takeoff) 3.0 (cruise)[d]	36.0 (takeoff) 14.3 (cruise)	16.0 (takeoff) 5.5 (cruise)
EI CO, g/kg	1.0	14.0 (idle)	73.0 (idle)	20.0 (idle)
EI HC, g/kg	0.5	2.0 (idle)	30.0 (idle)	1.0 (idle)
Combustion efficiency, %	$\geq$ 99.0	-----	99.9 (takeoff) 95.0 (idle)	$\geq$ 99.0 (idle and takeoff)
Total pressure loss, %	< 10.0	-----	4.3 (takeoff)	< 6.0

[a]All power levels.
[b]Tradeoff possible in 5-mode cycle. Data for T-2 class engine from Ref. 4.
[c]Data for G.E. CF6-50 engine from Experimental Clean Combustor Program, Phase II (Ref. 3).
[d]Potential standard, not now specified by EPA.

Table 2. JPL Mod 2 burner design specifications and comparison with typical production engine burner[a]

Specification item	Mod 2 burner[b]	Engine burner[b]
Air total pressure	30.39 x 10^5 N/m^2 (30 atm)	30.39 x 10^5 N/m^2 (30 atm)
Air total temperature	812 K (1460°R)	821 K (1477°R)
Air flow rate	4.6 kg/s (10 lbm/s)	103.4 kg/s (228 lbm/s)
Chamber reference velocity	18.3 m/s (60 ft/s)	25.9 m/s (85 ft/s)
Chamber dwell time (no recirculation)	5.0 ms	2.6 ms
Chamber L/D (shape)	2.0 (cylindrical)	3.0 (annular)
Combustion length	36.8 cm (14.5 in.)	34.8 cm (13.7 in.)
Combustion space rate[c]	0.88 x 10^6 J/hr-m^3-N/m^2 (2.4 x 10^6 BTU/hr-ft^3-atm)	2.2 x 10^6 J/hr-m^3-N/m^2 (5.9 x 10^6 BTU/hr-ft^3-atm)
Combustion equivalence ratio	LBO < ER <1.0	>1.0
Overall equivalence ratio	LBO < ER <1.0	0.34
Air split for cooling	N.A.	~30%
Air split for dilution	N.A.	~38%
Premix reference velocity	157.8 m/s (518 ft/s)	N.A.
Premix Mach number	0.28	N.A. (0.27 at compressor discharge)
Premix dwell time	2.0 ms	N.A.
Premix length	30.5 cm (12 in.)	N.A.

[a]G.E. CF6-50. Data from Ref. 2.
[b]Takeoff conditions.
[c]At jet fuel ER = 0.34.

Table 3. Summary of Mod 2 burner variations

Power condition	Run number	Overall configuration	Atomizer head	Premix section	Flameholder version	Ignitor location
Low	47,48,49	AL	L	Standard	H	Apex
	58	BL	L	Modified	R1	Apex
	62	C	C	Standard	R1	Apex
Cruise	52	AC	C	Standard	H	Apex
	53,54,55,56	C	C	Standard	R1	Apex
	57	BC	C	Modified	R1	Apex
Takeoff	59	CH	H	Standard	R1	Apex
	60	CH	H	Standard	R1	Skirt
	61	D	H	Standard	R2	Skirt
	63	E	H	Standard	R3	Skirt

Table 4. Experimental plenum air state conditions[a]

Air condition	Power level		
	Low	Cruise	Takeoff
Pressure, N/m^2(atm)			
Design	4.46×10^5 (4.4)	11.75×10^5 (11.6)	30.39×10^5 (30)
Test point average	4.22×10^5 (4.17)	12.09×10^5 (11.93)	30.11×10^5 (29.72)
Standard deviation from average	0.21×10^5 (0.21)	0.32×10^5 (0.32)	0.83×10^5 (0.83)
Temperature, K (°F)			
Design	455(360)	728(850)	812(1000)
Test point average	459(367)	727(849)	782(948)
Standard deviation from average	3(5)	3(5)	9(15)

[a]Values are based on average for all test points at each simulated power level.

APPENDIX A

THE HYDROGEN-ENRICHMENT CONCEPT AND ITS APPLICATION TO JET COMBUSTORS

The basis of the hydrogen-enrichment concept for providing low-temperature combustion stems from experimental observations that admixtures of hydrogen with HC/air mixtures so depress the lean flammability limit that burning can take place at ultralean combined fuel-to-air ratios. The potential reduction in lean limits provided by such "tertiary" mixtures can be illustrated by the use of Le Chatelier s formula which predicts the lean limit of any mixture of fuel gases from a knowledge of the lean limits for the individual fuel gases. This formula is

$$L = \frac{100}{\frac{P_1}{N_1} + \frac{P_2}{N_2} + \cdots \frac{P_n}{N_n}} \qquad \text{(A-1)}$$

where

L = volume percent of total fuel gas in a lean limit mixture with air

$P_{1\cdots n}$ = volume percent of each combustible gas present in the fuel gas, calculated on an air- and inert-free basis so that $P_1 + P_2 + P_n = 100$

$N_{1\cdots n}$ = volume percent of each combustible gas in a lean limit mixture of the individual fuel gas and air

Equation (A-1) can be rearranged and expressed in terms of fuel/air mass ratios for more convenient use. For H_2/JP mixed fuels, Eq. (A-1) then becomes

$$R_{LM} = \frac{R_{LJP}}{1 + \beta_L F} \qquad \text{(A-2)}$$

where

R_{LM} = mass ratio of total fuel ($= \dot{M}H_2 + \dot{M}JP$) to air ($\dot{M}A$) in a lean limit mixture with air

F = mass fraction of H_2 in the fuel mix ($= \dot{M}H_2/(\dot{M}H_2 + \dot{M}JP)$

R_{LJP} = mass ratio of JP fuel to air in a lean limit mixture with air

$\beta_L = \frac{R_{LJP}}{R_{LH_2}} - 1$; with R_{LH_2} being analogous to R_{LJP}

Furthermore, it can be shown that the stoichiometric fuel/air mass ratios for the H_2/JP mixed fuels can be expressed in the same form as Eq. (A-2):

$$R_{SM} = \frac{R_{SJP}}{1 + \beta_S F} \tag{A-3}$$

where

R_{SM} = mass ratio of total fuel to air in a stoichiometric mixture with air

R_{SJP} = mass ratio of JP fuel to air in a stoichiometric mixture with air

$\beta_S = \frac{R_{SJP}}{R_{SH_2}} - 1$, with R_{SH_2} being analogous to R_{SJP}

Dividing Eq. (A-2) by Eq. (A-3), substituting $\dot{M}H_2/(\dot{M}H_2 + \dot{M}JP)$ for F, and rearranging permits expressing the system flow rate ratios required to satisfy particular lean limit equivalence ratios. Thus,

$$\left[\frac{\dot{M}JP}{\dot{M}H_2}\right]_{LM} = ER_{LM} \times R_{LJP}\left[\frac{\dot{M}A}{\dot{M}H_2}\right] - (1 + \beta_L) \tag{A-4}$$

Also, using the standard definition of operating equivalence ratio,

$$ER = \frac{\dot{M}H_2 + \dot{M}JP}{\dot{M}A \times R_{S\dot{M}}} \tag{A-5}$$

it can be shown that the system flow rate ratios in general are related to ER as follows:

$$\frac{\dot{M}JP}{\dot{M}H_2} = ER \times R_{SJP}\left[\frac{\dot{M}A}{\dot{M}H_2}\right] - (1 + \beta_S) \tag{A-6}$$

Taking the molecular weight of JP-5 as 170 and its H/C ratio as 2.0, and using flammability limits based on Bureau of Mines Bulletin 503 for H_2 and kerosene of 4.0% and 0.7% by volume, respectively, evaluation of Eqs. (A-4) and (A-6) yields the results plotted as solid lines in Fig. A-1 for several selected air-to-hydrogen mass ratios.

The solid line plots shown in Fig. A-1 form a useful "operating map" for conducting mixed-fuel experiments. For a given simulated power condition, the air mass flow rate through the combustor is nearly constant. Therefore, operation along a selected line of constant $\dot{M}A/\dot{M}H_2$ requires a minimum of H_2 flow rate changes since a large range of equivalence ratio can be covered by adjustments in jet-fuel flow rate only. This scheme has been adopted in the present JPL experiment as a matter of convenience.

Of course, the prediction of the Le Chatelier formula presumes homogeneously premixed, gas phase reactants. Moreover, it is noted that Bureau of Mines lean limits are influenced by direction of flame propagation relative to the laboratory combustion tube as well as by initial temperature and pressure, the latter effects generally being counteractive. Finally, lean flammability limits for the individual fuel gases (measured under quiescent conditions) and mixtures of them are essentially ideal limits where flame speed and, hence, flame stability go to zero. Therefore, the characteristics of practical significance for a lean-burning jet combustor intended to control pollutant emissions are its lean operating limits for efficient, stable combustion; i.e., the minimum operating equivalence ratios that yield CO and unburned HC emissions that are within acceptable levels. Obviously, those operating points that also yield acceptable NO_x emission levels as well as sufficient heat release for turbine requirements form the actual operating regime of overall acceptability.

The success of a combustor design in exhibiting acceptable operating limits, as defined above, cannot be reliably predicted a priori; hence, they must be determined experimentally. Nonetheless, the calculated ideal flammability limits are important because, with all other combustor factors fixed, fuels or fuel mixes with substantially lower ideal limits can be expected to provide significantly leaner operating limits.

The dashed lines in Fig. A-1 show, in a conceptual sense, additional rich and lean operational boundaries which together with the ideal flammability limit line illustrate the potential benefits of using hydrogen enrichment for achieving acceptable lean-burning combustor operation. The illustration is for a typical subsonic-cruise power condition for a 30:1 compression ratio, high-bypass turbofan engine.

Two selected rich boundary lines are shown in Fig. A-1. One is based on the NO_x emission goal of the present work of 1.0 g NO_2/kg of total fuel and the other is based on 3.0 g NO_2/kg of total fuel that has been suggested as a standard for cruise operation. The upper and lower end points of the boundary lines were evaluated for kinetically controlled NO_x production in one-dimensional flow with a 10.0-ms dwell time, using 100% jet fuel and 100% H_2, respectively. The data for intermediate mixed-fuel composition were interpolated for illustrative purposes. Both of these rich operating boundaries fall to the lean side of the ideal flammability limit for jet fuel alone.

Now, less dwell-time in the combustor, early-quench techniques, and the use of other values of predicted lean flammability limits would modify the placement of the rich boundary relative to the jet-fuel lean limit to some degree. But the fact remains that the temperature reduction needed for ultralow NO_x emission levels requires that the heat release reaction take place at equivalence ratios approaching the limit for jet-fuel/air combustion under jet combustor inlet conditions. Hence, at best, a low margin of acceptable flame stability, ignition, and combustion efficiency can be expected without some form of combustion aid. By virtue of its unique lean burning qualities, molecular hydrogen substituted for a portion of the jet fuel can provide a significantly improved margin.

The lean operating boundary shown in Fig. A-1 (to its interception of the ideal lean limit line) represents the line of constant adiabatic flame temperature (1407 K or 2073°F) typically required for cruise power. This boundary line, then, portrays that there is a minimum allowable premixed equivalence ratio that satisfies power requirements. But, since air-film cooling and perhaps secondary-air injection for temperature pattern-factor adjustment will be required in an engine combustor, the useful lean boundary will lie possibly 20 to 30% to the right of that shown. Note that cooling requirements should be much reduced from current practice due to the ultralean (cooler) burning zone.

Thus, the conceptual, acceptable operating regime with H_2-enrichment is enclosed by the lean and rich operating boundaries, the ideal flammability limit line, and the abscissa which represents pure H_2 fuel. The practical feasibility of applying the concept is the objective of the present work.

The experimental data point shown in Fig. A-1 is discussed in the body of this report and represents an operating condition demonstrated with the Mod 2 burner that satisfies all the ultralow-emission goals. The position of the data point relative to the lean operating boundary would permit about 20% of the air mass flow to be used for cooling and/or dilution.

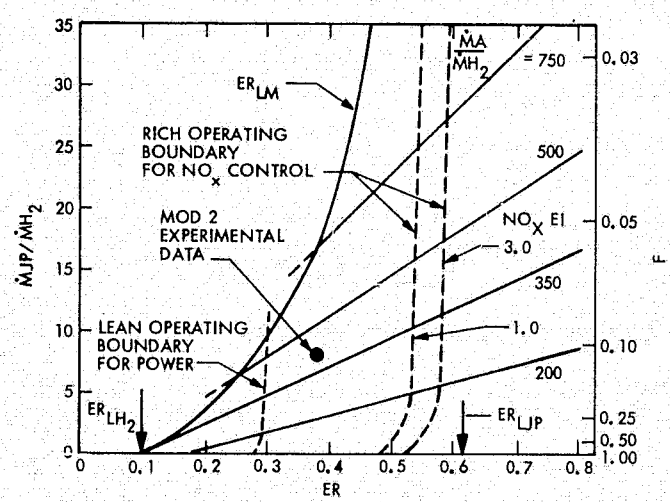

Fig. A-1. Operating map for hydrogen-enrichment concept. Operational boundaries depicted for cruise power; inlet air at 11.75 x 10^5 N/m^2 (11.6 atm), 728 K

APPENDIX B

DESCRIPTION OF TEST FACILITY AND SUMMARY OF THE INITIAL (MOD 1 BURNER) EXPERIMENTS

I. TEST FACILITY

The test facility used for the jet combustor experiments is located adjacent to the JPL hypersonic wind tunnel and is supplied with unvitiated, preheated air from the wind tunnel compressor plant, via the tunnel air heater. The present combustion test cell equipment and air-supply plumbing are rated to 34.44×10^5 N/m^2 (34 atm) pressure at 812 K (1000°F), although the compressor system to the heater outlet is rated to 49.64×10^5 N/m^2 (49 atm) at 939 K (1230°F). Air mass flow rates to approximately 6.8 kg/s (15 lbm/s) are available when the cited state conditions are achieved simultaneously. A schematic diagram of the overall air flow circuit is shown in Fig. B-1.

The test cell is equipped with conventional water, fuel (N_2-pressurized 2.3-m^3 (600-gal) tank), ventilation, and pressurant services, as well as a high-pressure bottled-H_2 supply (1274 m^3 or 45,000 SCF). A control room located adjacent to the test cell permits remote operation of the cell by means of electric and pneumatic controls. Tests can be monitored via closed-circuit TV. The compressor plant and air heater are controlled from a separate operator console through voice communication with the combustion test cell operator.

A high-pressure, cylindrical burner housing, shown schematically in Fig. B-2, normally houses the test burner apparatus. This housing also provides essentially stagnated air to the entrance of the combustor by means of a flow diffuser and two perforated baffle plates located at the inlet end of the housing. Burner apparatus approaching 0.48 m (19 in.) in diameter and 1.8 m (6 ft) in length can be accommodated within the housing. A flanged end-dome fitted with a replaceable water-cooled nozzle provides for access to the test apparatus as well as combustion pressure control. Access ports for instrumentation and fuel lines are also fitted to the end-dome.

Air flow rates are measured with either sonic-flow nozzles or subsonic, sharp-edge orifices located in the air supply line just upstream of the entrance to the burner housing. Standard ASME practices are followed in meter design and primary measurement techniques. Nitrogen and hydrogen flows are similarly measured upstream of the entry of the respective flow circuits to the burner housing. Jet fuel flow rate is measured with a selection of turbine meters of appropriate size ranges located upstream of a remotely controlled throttle valve.

Data acquisition centers on a remotely located digital recording system connected to test measurements through a patch panel in the test cell control room. A number of strip chart data displays, as well as real-time digital display of any recorded channel, are available in the control room. The latter displays also include all computed mass flow rates and mixture ratios, as well as emission concentrations. The essentials of the instrumentation system are shown in the block diagram of Fig. B-3.

A description of the combustion gas sample probe and sample analysis used in these experiments is given in Section II-C.

II. MOD 1 BURNER EXPERIMENTS

The information contained here briefly summarizes the unpublished results of the initial JPL combustion experiments on evaluating the feasibility of using H_2-enrichment of jet fuel to achieve low emission burning in a continuous flow combustor. Experimental difficulties were encountered during these initial experiments that limited the results to a small range of test conditions at only the low power level (inlet air: average pressure = 4.15×10^5 N/m^2 (4.1 atm), average temperature = 457 K, or 363°F).

The experiments were conducted with a burner assembly now designated as Mod 1. The same facilities, procedures, instrumentation system, and gas-sample analysis system described for the Mod 2 experiments were used. Jet fuel (JP-5) and gaseous H_2 were utilized.

The version of the Mod 1 burner with which emissions data were obtained is shown schematically in Fig. B-4. For this burner the H_2 was injected subsonically at the inlet to the mixing section through the injector shown in Fig. B-5. It was intended that the H_2/air mixing be nearly completed at the station of jet-fuel injection by virtue of the well-dispersed H_2 injection orifices. The contraflow orientation of jet-fuel injection from the pneumatic atomizer (same design as used in the Mod 2 burner, except for H_2 injection) was intended to introduce a well-dispersed, fog-like spray into the oncoming mixture and to enhance the mixedness of all reactants before they entered the flameholding region downstream of the annular "V" gutter. It turned out, however, that this mixing section design was inadequate to prevent flashback and subsequent flameholding upstream of the flameholder when H_2 was used, though this problem was not observed with jet-fuel-only operation.

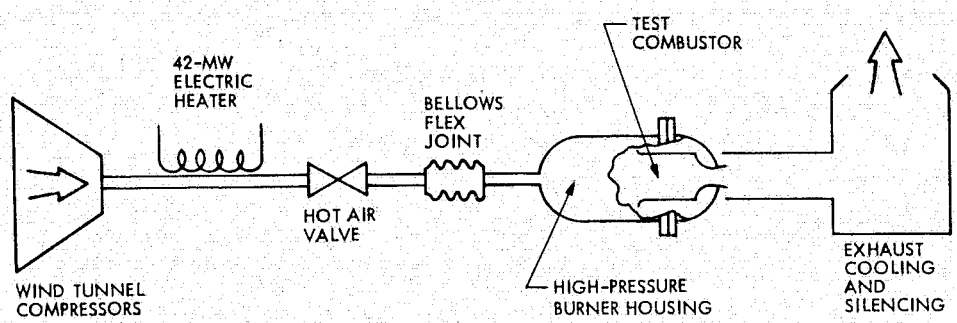

Fig. B-1. Overall air flow circuit of test facility

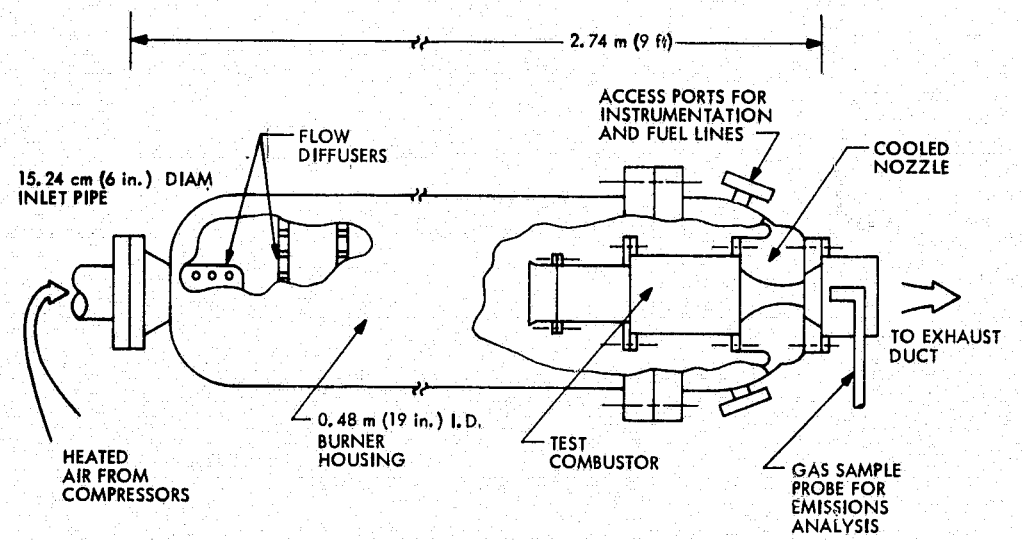

Fig. B-2. Schematic diagram of burner housing

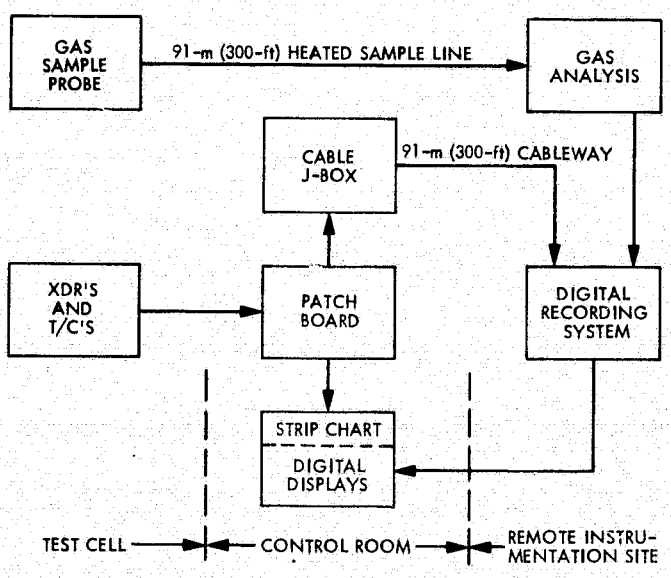

Fig. B-3. Block diagram of instrumentation system

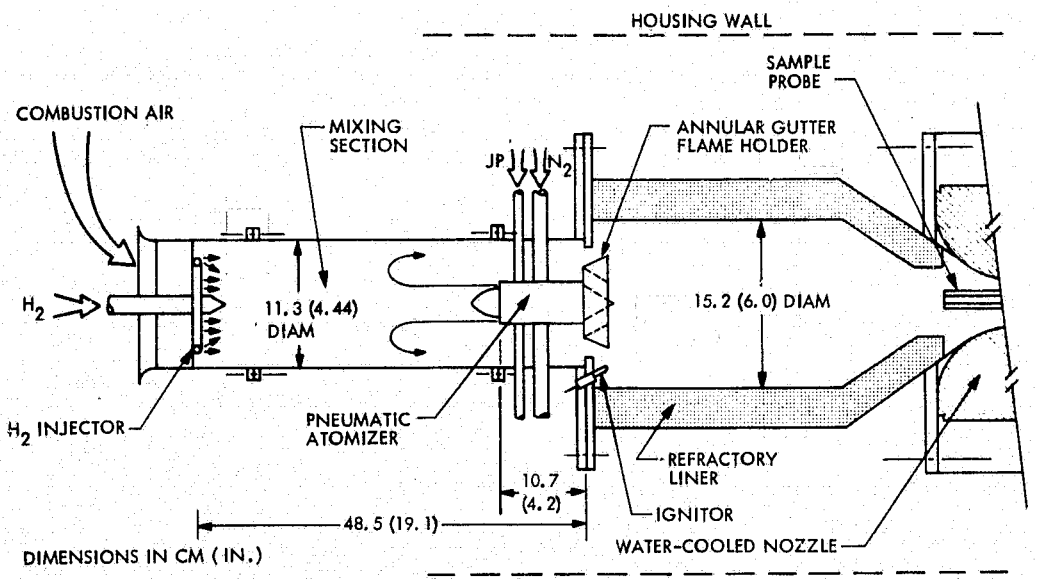

Fig. B-4. Mod 1 burner assembly schematic

Several modifications to the above arrangement were tried, within the constraints of the basic design, without success before terminating the initial experiments. At that time, it was concluded that the problem was the result of two deficiencies:

1. Insufficient margin of space velocity in the mixing section to account for transient conditions during ignition whenever combustion pressure increased momentarily. The steady-state design velocity (at low power) of about 21 m/s (70 ft/s) was estimated to decrease to near zero momentarily during ignition. And, since H_2 was being used for ignition, a H_2 flame would stabilize around the H_2 jet-flow region just downstream of the H_2 injector as a result of momentary flashback from the combustion chamber. This flame could be extinguished by terminating the H_2 flow, and jet-fuel-only operation would then proceed without upstream burning. However, if H_2 flow were restarted, the pressure pulse in the combustor was sufficient to cause reignition at the H_2 injector.

2. Too many flow disturbances in the mixing section. Inspection of Fig. B-4 shows that both the H_2 injector and the jet-fuel atomizer with its support struts provided flow disturbances amenable to flame stabilization, given an ignition source. Thereafter, the relatively low level of steady-state velocity in the mixing section was inadequate to "blow out" the locally stabilized flame.

The redesign to correct these deficiencies resulted in the Mod 2 burner described in the body of this report. To date, there has been no recurrence of upstream flame-holding with the revised design, although flameholder durability has been a problem.

The emissions data obtained with the Mod 1 burner are shown in Figs. B-6 and B-7. The variables presented in the figures have the same definition as those used in Section III of this report. The limited range of experimental conditions does not permit a precise determination of slope changes for all data, but the extension of the lean operating limit is clearly demonstrated by the comparison of the trends of the CO and HC emissions for jet-fuel-only and mixed-fuel data in Fig. B-6. The interpretation of these trends is that 10-15% H_2-enrichment significantly suppressed the onset of the typical rapid rise in CO and HC under very lean conditions. Combustion efficiency averaged a nearly constant 97% over the ER range shown in Fig. B-6.

The NO_x emissions are compared to calculated results based on chemical kinetics in Fig. B-7. While precise agreement would not be expected, it is clear that the trend of the data does not show as rapid a decrease of NO_x with decreasing equivalence ratio as the calculated results.

Two coupled factors are believed to have caused the higher-than-expected NO_x emissions for mixed-fuel operation: (1) upstream burning in the mixing section, and (2) that burning taking place at richer than the input equivalence ratio. The first effect would increase NO_x in nearly direct proportion to increased residence time of the hot combustion products and the second effect would increase NO_x exponentially with temperature. These interpretations are consistent with the generally closer agreement of the emissions data for jet fuel only with the kinetic estimates.

Thus, the Mod 1 burner failed to yield the ultralow emission and performance goals of this program, but it served to demonstrate the basic benefits of H_2-enrichment in a preliminary way. Of course, the potential problems of using premixed H_2 were also demonstrated in this deficient burner design.

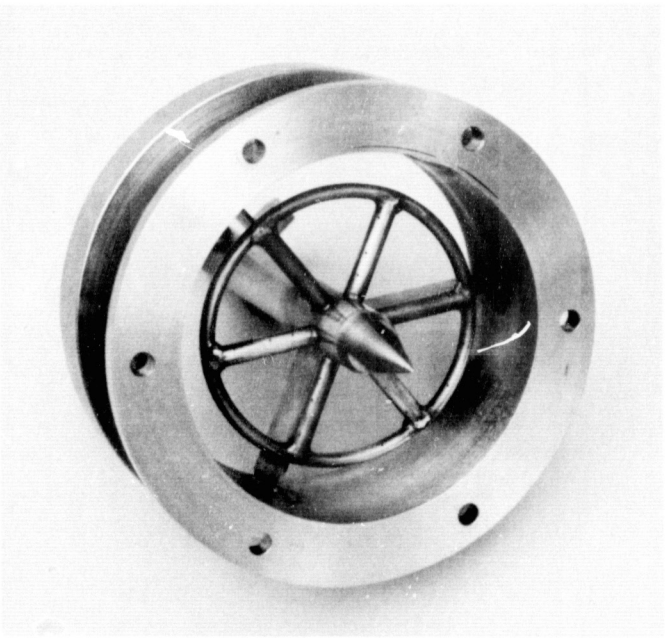

Fig. B-5. Mod 1 hydrogen injector

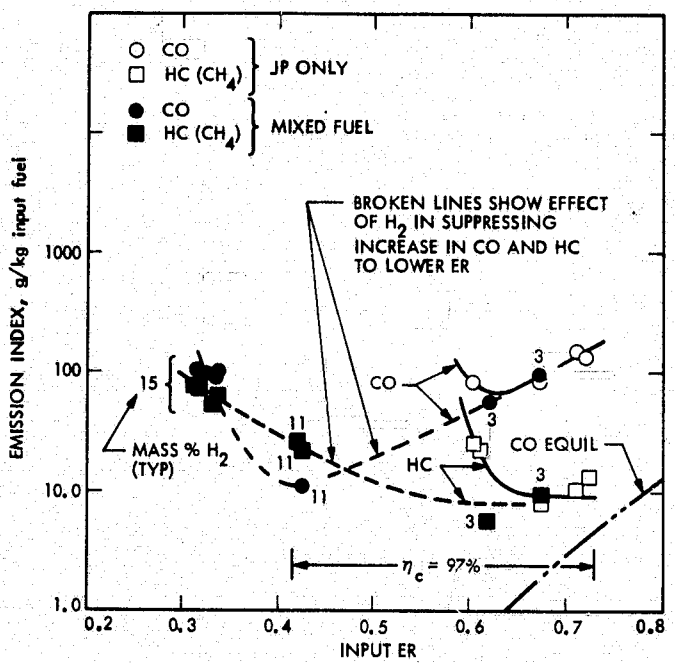

Fig. B-6. Mod 1 burner low power CO and HC emissions. Inlet air: 4.15 x 10^5 N/m^2 (4.1 atm), 457 K (363°F)

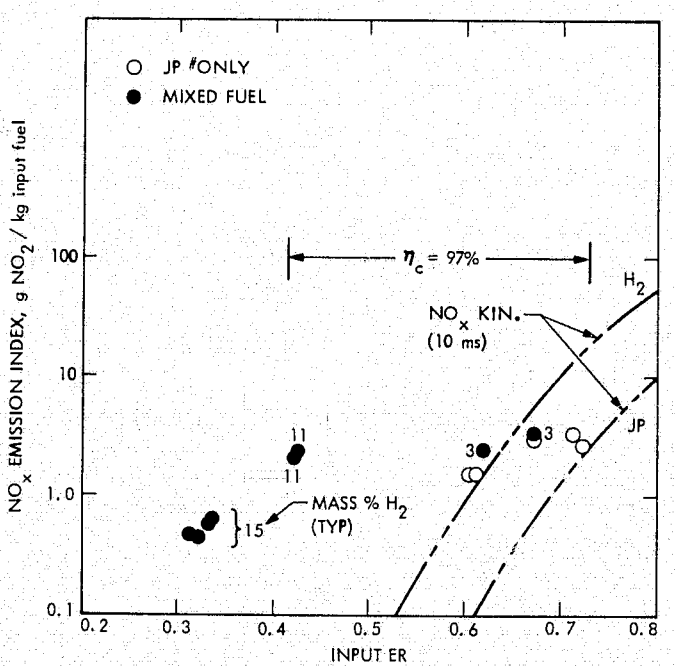

Fig. B-7. Mod 1 burner low power NO_x emissions. Inlet air: 4.15 x 10^5 N/m^2 (4.1 atm), 457 K (363°F)

APPENDIX C

CALCULATION PROCEDURES

I. PARAMETERS BASED ON MEASURED INPUT FLOWS

A. EMISSION INDEX

$$EI_p = ppm_p \times \bar{M}_p \times \left(1 + \frac{\dot{M}A}{\dot{M}F_t}\right) \times 10^{-3}$$

where

ppm_p = measured volumetric concentration in parts per million of pollutant p in dry gas sample

$\bar{M}_p$ = ratio of molecular weights of pollutant p to exhaust gas, taken as

$\bar{M}_{HC}$ = 0.5585 (expressed as CH_4)

$\bar{M}_{CO}$ = 0.9773

$\bar{M}_{NO_x}$ = 1.6056 (expressed as NO_2)

$\dot{M}A$ = measured mass flow rate of air to combustor

$\dot{M}F_t$ = measured mass flow rate of total fuel to combustor ($\dot{M}H_2 + \dot{M}JP$)

Note: Neglecting the atomizer N_2 flow in calculating EI_p nearly compensates for the H_2O removed from the sample before analysis. Thus, EI_p is equivalent to wet basis analysis to within a few percent. NO absorption by the separated water was determined to be negligible.

B. EQUIVALENCE RATIO

$$\text{Input ER} = \frac{\dot{M}F_t/\dot{M}A}{R_{SM}} = \frac{1}{\dot{M}A}\left(\frac{\dot{M}JP}{R_{SJP}} + \frac{\dot{M}H_2}{R_{SH_2}}\right) = \text{INPUT JP ER} + \text{INPUT } H_2 \text{ ER}$$

where

R_{SM} = stoichiometric mixed-fuel to air ratio

$$= \frac{R_{SJP}}{1 + \beta_S F}$$

R_{SJP} = stoichiometric JP-5 to air mass ratio, taken as 0.06763

$\beta_S = \frac{R_{SJP}}{R_{SH_2}} - 1$, with R_{SH_2} taken as 0.02916

F = mass fraction of H_2 in total input fuel mix.

C. COMBUSTION EFFICIENCY, %, (ASSUMING COMPLETE H_2 COMBUSTION)

$$\eta_c = 100 - \left[\frac{Q_{CO} \times EI_{CO} + Q_{CH_4} \times EI_{HC}}{10\left(Q_{JP} + F\,(Q_{H_2} - Q_{JP})\right)}\right]$$

where

Q = lower heating value for specific reactants

Q_{CO} = 1.007×10^7 J/kg (4344 BTU/lbm)

Q_{CH_4} = 4.986×10^7 J/kg (21,502 BTU/lbm)

Q_{JP} = 4.267×10^7 J/kg (18,400 BTU/lbm)

Q_{H_2} = 11.958×10^7 J/kg (51,571 BTU/lbm)

II. PARAMETERS BASED ON SAMPLE COMPOSITION

A. DEFINITIONS

Hydrocarbon = X ($CH\alpha$), where X = moles of $CH\alpha$ equivalent to total moles of $C_nH\alpha_n$

Air (1 mole) = .2095 O_2 + .7809 N_2 + .0093 Ar + .0003 CO_2

Atomizer N_2 = βX, where β = measured input N_2-to-jet fuel volumetric ratio.

Then

$$X(CH\alpha) + Y(H_2) + Z(Air) + \beta X(N_2) \rightarrow A(CO_2) + B(CO) + C(CH\alpha) + D(NO) + E(H_2O) + G(O_2) + I(N_2) + J(Ar)$$

Setting A + B + C + D + E + G + I + J = T, and since the product species are measured as dry volumetric fractions,

$$[CO_2] = \frac{A}{T - E}, \quad [CO] = \frac{B}{T - E}, \quad [CH\alpha] = \frac{C}{T - E}, \quad [NO] = \frac{D}{T - E}, \quad [O_2] = \frac{G}{T - E}$$

Also,

$$\dot{M}F_t = \dot{M}H_2 + \dot{M}JP = X\,(M_c + \alpha M_H) + Y(M_{H_2})$$

and

$$\dot{M}A = Z(M_A)$$

where all molar coefficients are taken as volumetric flow rates, and

M_C = atomic weight of carbon = 12

M_H = atomic weight of hydrogen = 1

M_{H_2} = molecular weight of hydrogen = 2

M_A = molecular weight of air = 28.97

α = jet fuel H/C ratio (assumed) = 2

B. REACTANT VOLUMETRIC RATIOS

Using the foregoing definitions and the approximations that measured total unburned HC = $[CH\alpha]$ and measured NO_x = [NO], the following intermediate relationships can be derived for computing parameters based on sample measurements of $[O_2]$, $[CO_2]$, [CO], [HC], and $[NO_x]$, which are volumetric concentrations (expressed in percent).

$$\frac{Y}{X} = e = \frac{ac - d}{b - .0003a}$$

where

$$a = \frac{100 - (1 + 2\beta)b - \frac{[NO_x]}{2} - [O_2]}{.7902 - .0006\beta}$$

$$b = [CO_2] + [CO] + [HC]$$

$$c = \text{constant} = \frac{.0003\alpha}{2} + .4196 = .4199$$

$$d = \frac{(2 + \alpha)}{2}[CO_2] + \frac{(1 + \alpha)}{2}[CO] + [NO_x] + 2[O_2]$$

$$= 3[CO_2] + 2[CO] + [NO_x] + 2[O_2]$$

Also,

$$\frac{Y}{Z} = c\,\frac{d}{a} = .4199\,\frac{d}{a}$$

$$\frac{X}{Z} = \frac{b}{a}\,.0003$$

C. REACTANT MASS RATIOS

From the volumetric relationships and the previous definitions of ER and F, the following sampled reactant mass ratios can be derived.

$$\text{Sample F} = \frac{Y(M_{H_2})}{Y(M_{H_2}) + X(M_C + \alpha M_H)} = \frac{e}{e + 7}$$

$$\text{Sample JP ER} = \left(\frac{M_C + M_H}{R_{SJP}\,M_A}\right)\left(\frac{X}{Z}\right) = 7.146\left[\frac{b}{a} - .0003\right]$$

$$\text{Sample } H_2 \text{ ER} = \left(\frac{M_{H_2}}{R_{FH_2}\,M_A}\right)\left(\frac{Y}{Z}\right) = 2.368\left[.4199\,\frac{d}{a}\right]$$

$$\text{Sample ER} = \text{Sample JP ER} + \text{Sample } H_2 \text{ ER}$$

D. EMISSION INDEX

Also, from the foregoing and from the basic definition of Emission Index

$$EI_p = \frac{\text{mass units of pollutant species}}{\text{1000 mass units of fuel}}$$

the following general expression for sampled EI can be derived.

$$EI_p = \frac{M_p \times P' \times 10^3 [X - .0003Z]}{[X(M_C + \alpha M_H) + YM_{H_2}] [b]}$$

$$= M_p \times P' \times 10^3 \times g$$

where

P' = measured volumetric concentration of pollutant species p

M_p = molecular weight of pollutant species p

$$g = \frac{(b - .0006a)/(b - .0003a)}{b(14 + 2e)}$$

Note: e was arbitrarily set to zero when H_2 was not used.

Assigning the values $M_{NOx} = 46$ (expressed as NO_2), $M_{CO} = 28$, and $M_{HC} = 14$ (expressed as $CH\alpha$) and expressing P' as ppm_p, the following expressions for specific pollutants are obtained.

$$EINO_x = 4.6 \times ppm_{NO_x} \times g$$

$$EICO = 2.8 \times ppm_{CO} \times g$$

$$EIHC = 1.4 \times ppm_{HC} \times g$$

III. CONVERSION TO EQUIVALENT JET FUEL

For those mixed-fuel data presented on the basis of equivalent jet fuel the following transformation procedure was used to approximate combustion ΔT equivalency. Assuming constant heat capacities and 100% combustion,

$$\frac{R_{JP}\, Q_{JP}}{R_{JP} + 1} = \frac{R_M\, Q_M}{R_M + 1}$$

where

R_{JP} = jet-fuel to air ratio producing ΔT equivalent to that produced by R_M

R_M = mixed-fuel to air ratio deduced from sample composition

$Q_M = Q_{JP} + F(Q_{H_2} - Q_{JP})$

Thus, after manipulation and substitution of previously assigned values for Q_{JP} and Q_{H_2},

$$R_{JP} = \frac{R_M(1 + 1.803F)/(R_M + 1)}{1 - R_M(1 + 1.803F)/(R_M + 1)}$$

and

$$ER \text{ (JP equivalent)} = \frac{R_{JP}}{R_{SJP}} = 14.79\ R_{JP}$$

Emission Index as calculated from the gas sample was also converted to an equivalent JP basis:

$$(EI_p)_{JP \text{ equivalent}} = EI_p \left(\frac{R_M}{R_{JP}} \right)$$

NASA—JPL—Coml., L.A., Calif.